solar

MDPI

Review

A Review of Photovoltaic Module Failure and Degradation Mechanisms: Causes and Detection Techniques

Hussain Al Mahdi [1], Paul G. Leahy [2], Mohammad Alghoul [3] and Alan P. Morrison [1,*]

[1] Electrical & Electronic Engineering, School of Engineering & Architecture, University College Cork, T12 K8AF Cork, Ireland; 118225936@umail.ucc.ie
[2] Energy Engineering, School of Engineering & Architecture, University College Cork, T12 K8AF Cork, Ireland; paul.leahy@ucc.ie
[3] Interdisciplinary Research Centre for Renewable Energy and Power Systems (IRC-REPS), King Fahd University of Petroleum & Minerals, Dhahran 31261, Saudi Arabia; mohammad.alghoul@kfupm.edu.sa
* Correspondence: a.morrison@ucc.ie

Abstract: With the global increase in the deployment of photovoltaic (PV) modules in recent years, the need to explore and understand their reported failure mechanisms has become crucial. Despite PV modules being considered reliable devices, failures and extreme degradations often occur. Some degradations and failures within the normal range may be minor and not cause significant harm. Others may initially be mild but can rapidly deteriorate, leading to catastrophic accidents, particularly in harsh environments. This paper conducts a state-of-the-art literature review to examine PV failures, their types, and their root causes based on the components of PV modules (from protective glass to junction box). It outlines the hazardous consequences arising from PV module failures and describes the potential damage they can bring to the PV system. The literature reveals that each component is susceptible to specific types of failure, with some components deteriorating on their own and others impacting additional PV components, leading to more severe failures. Finally, this review briefly summarises PV failure detection techniques, emphasising the significance of electrical characterisation techniques and underlining the importance of considering more electrical parameters. Most importantly, this review identifies the most prevalent degradation processes, laying the foundation for further investigation by the PV research community through modelling and experimental studies. This allows for early detection by comparing PV performance when failures or degradation occur to prevent serious progression. It is worth noting that most of the studies included in this review primarily focus on detailing failures and degradation observed in PV operations, which can be attributed to various factors, including the manufacturing process and other external influences. Hence, they provide explanations of these failure mechanisms and causes but do not extensively explore corrective actions or propose solutions based on either laboratory experiments or real-world experience. Although, within this field of study, there are corresponding studies that have designed experiments to suggest preventive measures and potential solutions, an in-depth review of those studies is beyond the scope of this paper. However, this paper, in turn, serves as a valuable resource for scholars by confining PV failures to critically evaluate available studies for preventative measures and corrective actions.

Keywords: PV module failure; PV module degradation; failure detection; degradation monitoring; failure mechanisms; degradation mechanisms; PV module lifetime

Citation: Al Mahdi, H.; Leahy, P.G.; Alghoul, M.; Morrison, A.P. A Review of Photovoltaic Module Failure and Degradation Mechanisms: Causes and Detection Techniques. *Solar* **2024**, *4*, 43–82. https://doi.org/10.3390/solar4010003

Academic Editors: Philippe Poure and Shamsodin Taheri

Received: 26 October 2023
Revised: 22 December 2023
Accepted: 4 January 2024
Published: 9 January 2024

1. Introduction

Among different renewable energy sources, solar energy is the most prevalent renewable source in most regions of the world due to its cost-effective implementation and simple installation [1]. The cost of photovoltaic (PV) systems has declined rapidly over time [2]. Between 1990 and 2020, Germany's PV investment for a 10 kW system dropped by nearly

92.6% from EUR 14,000 to EUR 1036 per kW [3]. In the U.S., the decline in the wholesale price for multi-crystalline modules was roughly 95% between 2008 and 2018. Figure 1 shows the average annual addition of solar energy over other renewable energy sources for the past three years.

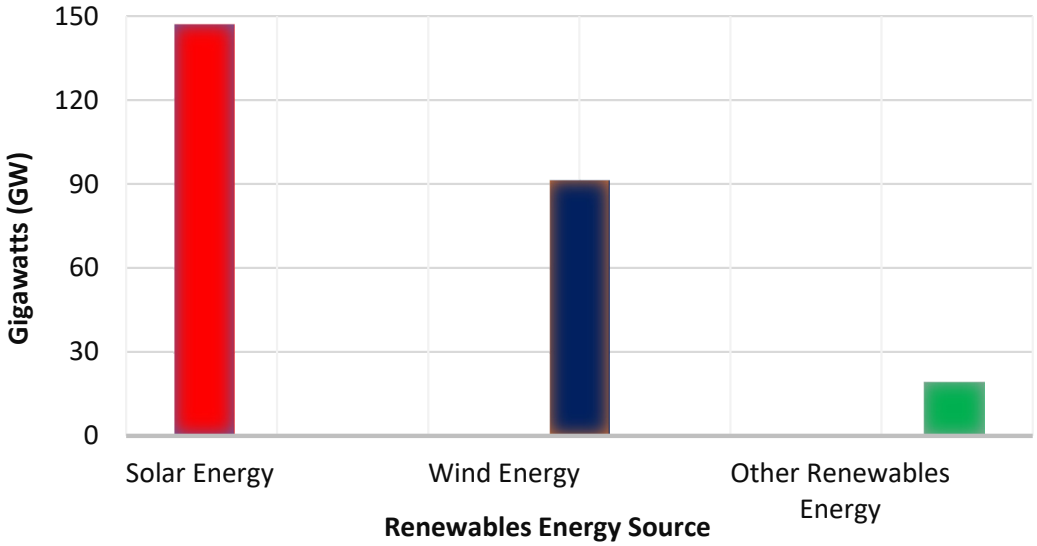

Figure 1. Average annual renewable capacity addition of renewable energy sources between 2020 and 2022 [4].

The conversion efficiency of the solar cell has progressed rapidly [5]; nowadays, it converts nearly 26% of the solar spectrum within the wavelength range from 350 nm to 1150 nm into electrical energy [6]. PV cells are serially connected to maximise energy production. Then, they are packaged into modules using a polymer coating, the encapsulant, and covered by a protective layer, predominantly made from glass [7,8]. After being encapsulated, the PV module is ready to use and guaranteed by manufacturers to have a 25-year lifetime with an expected degradation rate of 0.8% of power per annum [9–11]. This degradation rate was derived following extensive experimental studies and assessments that have been conducted. That is, failures found in previously deployed PV modules, such as encapsulant and solar cell defects, prompted the development of these studies. For instance, the National Renewable Energy Laboratory (NREL) developed accelerated stress tests to examine degradation rates, validating the superior quality and long-term reliability of PV modules [12]. However, despite these measures, there are still reports of abnormal degradation rates in PV modules due to a variety of failures. Abnormal degradation rates dramatically reduce reliability and increase the cost of PV operation. Harsh weather conditions and manufacturing defects are among the major factors influencing degradation rates. Consequently, higher degradation rates pose a barrier to favouring PV applications over other energy sources [13,14].

The need to review PV failures and degradation has encouraged researchers to engage in comprehensive research investigating and analysing experiments and real-world industry studies available in the literature. Köntges et al. [15] reviewed PV failures based on their emergence in the operational life cycle. Jordan and Kurtz [16] reviewed PV failures based on a severity scale, where Scale 1 referred to no effect on the PV system and Scale 10 referred to destructive effects on PV power that pose safety risks. Madeti and Singh [17] differentiated between reversible PV failures (temporary) such as shading from snow covering or dust accumulation and irreversible failures (permanent) such as encapsulant discolouration, reviewing applicable detection techniques on the DC and AC sides of the PV system. Pillai and Rajasekar [18] focused on detection techniques for PV failures and segregated failures based on their occurrence due to environmental stress factors and electrical (e.g., line to line, line to ground) and physical appearance, whether damaging the PV module or the

connected devices and accessories. A recent review by Osmani et al. [19] followed a similar direction as Pillai and Rajasekar [18], focusing more on detection techniques with limited exposure to the failure mechanisms occurring on the PV module. Despite the solid analysis in the aforementioned published reviews [15–19], the literature still lacks an in-depth state-of-the-art review that provides detailed information on failures encountered in the PV module itself and its components (from protective glass to backsheet), exploring their mechanisms and root causes.

In response, the review in this paper takes a different approach from other reviews by exploring and illustrating PV failures and degradation mechanisms based on PV module components. This review begins by evaluating the degradation rates reported in the literature in Section 1. In Section 2, it focuses on PV module failures and degradation mechanisms based on PV module components, incorporating a discussion and observation to identify the root causes of their occurrence and raise awareness of their consequences on safety and energy loss. Sections 3 and 4 provide a brief survey of the classification categories of PV failures and how they are affected by environmental stressors. This review concludes by discussing common detection techniques for PV failure and degradation mechanisms in Section 6. Future directions are proposed to explore available solutions and corrective actions to ensure the reliable and safe operation of PV generation, assisting PV investors in reducing revenue loss.

1.1. Degradation Rate

A study by Jordan et al. [20] examined PV modules that operated for 20 years and found the degradation rate was within the normal range; a 0.8% drop in the rated power per annum. However, several studies, e.g., [21–25], found that the degradation rate might vary depending on many factors such as material properties, environmental stress, installation, design and type of connections, and whether the PV system is connected to the electrical grid or standalone. Another study by Jordan et al. [26] examined several degradation rates from 40 countries; the findings agreed with [21–24] in that these factors significantly affect the degradation rate. It can be noted from Colvin et al. [27] that the median degradation rate of grid-connected PV systems was higher than that of standalone PV systems deployed in the years before 2000, but became lower after 2000. In addition, these factors were also described by Köntges et al. [15], including damage during transportation, which was found to degrade the PV module more rapidly.

Degradation rates of more than 1% per annum have been reported across PV modules deployed in India [28]. Previous to this, Quansah et al. [29] monitored PV modules that operated for 16 years in northern Ghana, particularly off-grid-connected, monocrystalline systems, and found that the annual degradation rate reached 1.54%. The average temperature of north Ghana could reach 30 °C, combined with an intermediate humidity level of 43%, which is close to the weather conditions in India. Degradation rates within these ranges represent double the expected loss in potential power generation. Table 1 lists the reported degradation rates from some recent studies.

Table 1. Degradation rates of PV systems reported within the last two years.

Degradation Rate	Type of PV (Poly-Si, Mono-Si)	Connection (Grid or Standalone)	Lifetime (Years)	Weather Condition	Country	Ref.
Between 0.9% and 1.1%. The rate increased to up to 5.9% with visible failure modes.	Poly-Si	Grid	6	Subtropical climate with moderate humidity level and high temperature.	India	[29]
Modules with no visual defect have around 1% whereas modules with defects may reach 4.2%.	Poly-Si	Grid	10	Semi-desert climate, considerably hot and dry weather.	India	[30]

Table 1. *Cont.*

Degradation Rate	Type of PV (Poly-Si, Mono-Si)	Connection (Grid or Standalone)	Lifetime (Years)	Weather Condition	Country	Ref.
0.6% to 1.2% for modules with no visual defect and 1.4% to 1.9% for modules with defects.	Mono-Si	Standalone	Between 0 and 5	Dry equatorial climate. The average temperature is 28 °C and 30 °C and the average humidity is between 60% and 75%.	Ghana	[31]
0.75% to 1.65% for modules with no visual defect and 1% to 2% for modules with defects.	Poly-Si	Standalone	Between 6 and 10.	Wet semi-equatorial climate. The average temperature ranges between 26 °C and 30 °C and the average humidity is between 70% and 80%.		
The average fluctuates from 0.92% to 1.05%. Modules with defects can reach 3.22%.	Mono-Si	Standalone	10	Hot accompanied by high relative humidity; up to 85.6%.	U.S.	[32]
1.54% in mono-si and 2.72% in poly-si.	Both Types	Standalone	11	Dry and hot climate, with frequent sandstorms located in the desert.	Algeria	[33]
The average rate of 20 deployed modules is 1.04%.	Mono-Si	Standalone	11	Warm with a high relative humidity range; the average is 67%.	Algeria	[34]
The average rate of 10 deployed modules is 2.04%.	Poly-Si	Standalone	14	Moderate climate with considerably high relative humidity, which can reach 83% in the winter months.	Germany	[35]
Between 0.57 and 1.33% based on extracted data and statistical analysis.	Poly-Si	Grid	5	Desert climate, considerably hot and dry. Frequent sandstorms result in dust accumulation on the PV system.	Djibouti	[11]
0.98%	Poly-Si	Not stated	10	Cold and humid, average temperature range between −6.7 °C and 21 °C, average humidity range between 30% and 99%.	Norway	[36,37]
1.33%	Poly-Si	Not stated	20	PV modules were operated for 10 years in humid and cold weather and then kept inside a research centre for 10 years for examination purposes.		

Furthermore, some PV failures, such as cell cracks, propagate rapidly [33,34]; if undetected, they will cause a significant cost loss that may reach up to 10 times the equipment cost [38]. This is because some undetected failures may lead to fire and catastrophic damage to the entire PV system [39]. For instance, critical degradation in some PV modules in an array system leads to mismatch, increasing the PV module's temperature and subsequently leading to fire [40,41]. Critical degradation in PV modules was also highlighted as initiating fire in a research project based in Germany [39]. Fire can also be caused by hotspot failure, primarily driven by other failure mechanisms that elevate the operating temperature to a hazardous level, and eventually cause a fire [42,43]. There have been 80 fire incidents

involving PVs in the United Kingdom alone [44]. The fire caused by PV failures not only results in power reduction and cost losses, but it may sadly lead to fatalities; twenty-two casualties related to fire incidents stemming from PV failures were reported in the UK by BRE National Solar Centre [44]. Additionally, hydrogen reactions during PV fires cause toxic and life-threatening gases, namely hydrogen fluoride and hydrogen chloride [45]. Figure 2 shows a fire incident triggered by a hotspot failure on a module in China.

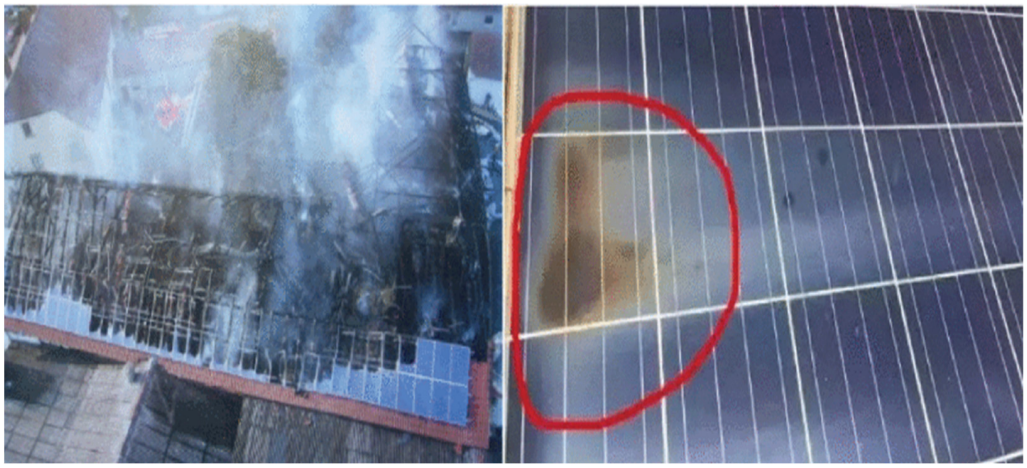

Figure 2. Fire incident in PV array initiated by hotspot failure [45].

According to Sepanski et al. [39], PV modules do not catch fire abruptly; fires are often sparked by critical degradation mechanisms that can be detected in advance.

1.2. Definition of PV Failure

Photovoltaic failure is not defined uniformly in the literature. Some definitions indicate that a drop of 80% in maximum output power is considered a PV failure [46]. Others claim a 20% drop in maximal power is a PV failure [47]. Durand and Bowling [48] defined failure as a drop of more than 50% in maximum power output. However, the International Electrotechnical Commission (IEC) stated that a 50% drop in maximum power output must be accompanied by safety hazards to ascertain failure in the PV module [49]. This discrepancy in defining the term explains the reason why Jordan et al. [16] used the term "degradation mode" instead of "failure" when reviewing the literature. Despite discrepancies in defining the "failure" term, the authors of this paper use both terms: failure and degradation. The term "failure" is universally described in the literature as any unusual changes in the PV module's appearance, function, and reliability [46,50], whereas the term degradation describes the wear-out process of the PV module during its ordinary life cycle. In most cases, the degradation process, if within the expected range of 0.8% drop of rated power per annum, does not harm the PV system unless it exceeds this range and moves to a critical phase [38,51].

2. Failures of the PV Module Components: Discussion and Observations

A PV module consists of solar cells, solder, an encapsulant, protective glass, and a backsheet, see Figure 3. The most common raw material for the PV cell is silicon. Although silicon is not the ideal element for power conversion efficiency, its properties have been extensively studied and well understood by the market before the development of solar cells [5,52].

Silicon is highly purified and drawn into single crystal ingots before being sliced into wafers ranging between 0.2 to 0.5 mm thick. Residuals of crystalline silicon created during the slicing process vary based on the slicing technology. They are frequently used as crystalline ribbons to reduce manufacturing costs [5]. Once the wafer is connected to the ribbon, the solar cell is ready for testing.

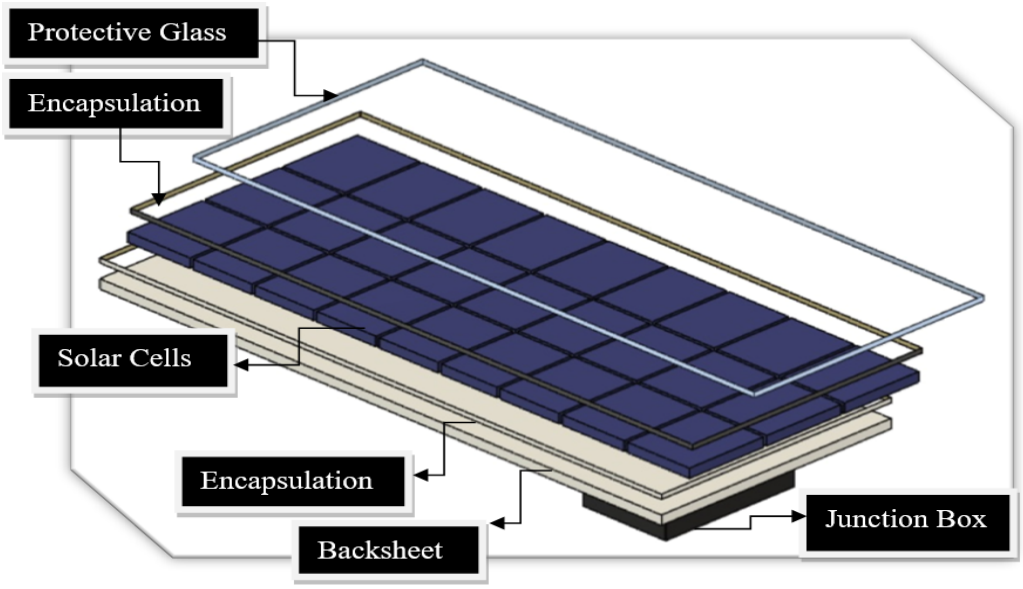

Figure 3. PV module components designed using Fusion 360 software. (The software is from Autodesk and is called Fusion 360. The version is 2.0 and Autodesk are located in San Francisco, CA, USA).

2.1. Protective Glass

The protective glass in the PV module is made from tempered glass that contains a small proportion of iron oxide, not exceeding 0.05%, to allow for the transmission of sun light [53]. It is manufactured and designed to resist environmental stress factors such as a drastic change in temperature.

Gürtürk et al. [54] validated glass properties by measuring its optical transmittance and energy efficiency. They investigated two types of PV glass, one of which was rated to have a 1% higher solar transmittance. One in each type was used as a control glass and tested at a constant temperature. The others were tested at an elevated temperature that reached 120 °C. Their results showed no significant impact on energy efficiency, only a slight variation, not exceeding 2.06% at most. Afridi et al. [55] artificially formed a hotspot via shading with temperature rising to 200 °C in glass/glass and backsheet/glass PV modules and proved that the front glass of those two types was not broken or shattered despite the occurrence of severe damage like burn marks, specifically in the glass/glass PV module type. Belhaouas et al. [34] inspected twenty PV modules equipped with two different types of glass after 11 years of deployment in Bouzareah, Algeria: eight with float glass and the other twelve with textured glass. Their visual inspection showed more optical failures such as delamination in the float glass types, albeit all PV modules suffered from discolouration. Moreover, the electrical parameters of PV modules with float glass type displayed reduced values compared to those with textured glass, except for the open-circuit voltage. Nonetheless, all twenty PV modules experienced nearly the same degradation rate, at 1.04% per year.

A reduction in light transmittance is the primary failure that occurs in PV glass and is potentially caused by glass breaking or shattering or by harsh weather conditions like ultraviolet exposure and dust accumulation [56,57]. A lab experiment by Tagawa et al. [58] explored dust accumulation on glass and its effect on transmittance. Their results revealed a dramatic coarseness increment that resulted in a 32% reduction in glass transmittance after 44 min of accumulation. To protect against harmful UV wavelengths, some PV glass is doped with cerium as an additive [59]. However, King et al. [60] discovered, in a laboratory experiment, that doping cerium reduces optical transmission by up to 2%. Kempe et al. [61] conducted further experiments on the impact of removing cerium from protective glass and found that excluding cerium can raise optical transmittance

by approximately 1.8% [18], which drives some manufacturers to abandon cerium in the production of PV glass. However, excluding cerium from PV glass is extremely risky; it can cause a substantial rise in the rate of delamination failure by a factor of three [61]. Consequently, when it comes to cerium, Kempe et al. [61] determined that excluding cerium will not boost electrical efficiency, and if excluded, there is a need to coat the glass with anti-reflective substances to filter out damaging ultraviolet wavelengths, predominantly below 350 nm.

Glass shattering can be the result of poor PV module transportation or incorrect manufacturing processes involving excessive clamping force [22,62–64]. Some weather conditions also contribute to PV glass degradation and failures. A study by Bora et al. [65] analysed the failure modes of PV modules in different weather conditions in India. They showed that PV modules deployed in hot areas were vulnerable to glass breakage within five years of operation. Shattering or breakage of the module's glass allows water vapor to enter the solar cells, creating short circuits and safety risks like electrical shock [30]. This is why glass breakage failure ranked 9 out of 10 in terms of severity as it affects safety severely [30].

In addition, the temperature at the glass's breaking point increases, which may cause hotspot failure [15]. In an investigation study by Chandel et al. [66], a PV module with glass breakage had developed hotspot failures with resulting significant power loss, which was also identified by Băjenescu and Titu-Marius [67]. Typically, a hotspot forms in a PV module when some cells receive less illumination than others, resulting in those cells dissipating energy rather than producing energy, i.e., the energy produced by the fully illuminated solar cells is dissipated by the less illuminated ones, increasing the latter cells' temperature and causing them to operate in reverse bias [68]. Hotspot failures are not only driven by broken glass failures but also driven by shading and mismatch failures [69]. Shading failure is a common PV failure that is strongly linked with hotspot formation [70,71]. When hotspots occur, they cause permanent damage to the solar cells or other module parts, such as metal connection, EVA encapsulation, or protective glass [72,73]. Jordan et al. [16] rated PV failures based on their severity, where one is low, and ten is considered the most severe; they listed hotspots to have the highest severity rate among all PV failures.

However, Ndiaye et al. [22] investigated a PV module with broken glass operating for five years and found no hotspot that led to significant power loss. This may indicate that glass breakage was not the cause of the failure, but a subsequent consequence due to weak protection. Bansal et al. [30] investigated a PV module operating for 10 years in a mega-plant and found that glass breakage was almost certainly combined with solar cell cracking and significant power loss as a result of weak protection, see Figure 4.

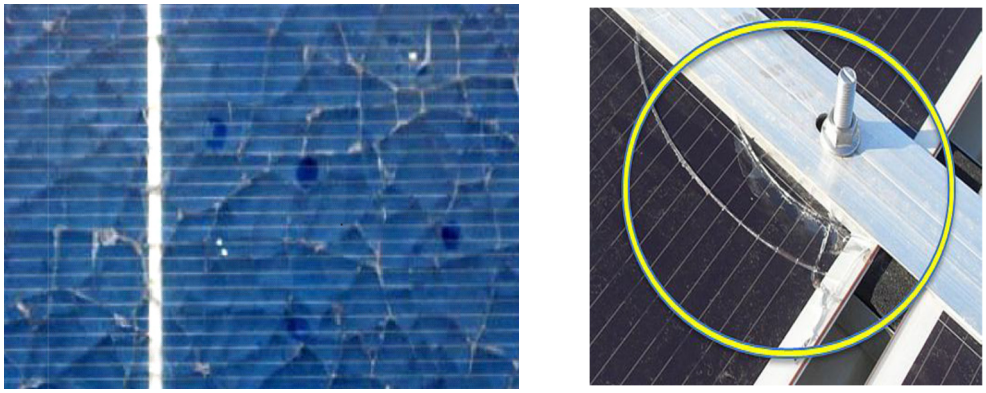

(**a**) (**b**)

Figure 4. (**a**) Example of PV module with shattered protective glass [74]. (**b**) Broken glass due to installation fault by over-tightening a bolt [15].

2.2. Encapsulant

Various encapsulating substances have been used in photovoltaic modules, such as polydimethylsiloxane (PDMS) and thermoplastic polyurethane (TPU) [8,75–77]. Manufacturers evaluate their advantages and disadvantages in terms of properties including reliability and cost before selection. For instance, PDMS demonstrates better immunity to environmental stress factors, which favoured it in the early trials of PV encapsulation [78]. Recently, manufacturers such as DuPont developed a PV encapsulant classified as an ionomer which offers 25 times more protection against potential-induced degradation (PID) failure than the typical encapsulant, ethylene-vinyl acetate (EVA). Dow Chemicals, another manufacturer, developed polyolefin-based encapsulants and has claimed they have greater electrical resistance as well as moisture protection when compared to EVA and ionomers [79,80]. Azam et al. [81] explored the degradation rate of four modules, two of which were laminated with polyvinyl butyral (PVB) encapsulant, under an accelerated ultraviolet test and found they had a 50% lower degradation rate compared to EVA.

Despite the superior protection features against environmental stress factors in more advanced encapsulating materials, EVA is still used in more than 75% of all PV modules due to its cost effectiveness [82,83]. The cost of PVB material, for instance, is about 50% more per m^2 than its competitor, EVA [81]. The majority of EVA composition is vinyl acetate, with the remainder being a combination of ethylene, antioxidants, and curing agents [84,85].

However, from the historical research carried out in 1981 by Lathrop et al. [86] at Clemson University until recent literature reviews, e.g., [87,88], EVA encapsulant is the primary cause of PV degradation mechanisms. Aboagye et al. [31] recently inspected polycrystalline and monocrystalline PV modules deployed in three locations in Ghana with different weather conditions, all of which showed defects in EVA encapsulants. The same findings were noted for 43 monocrystalline PV modules mounted for ten years in Nordic weather conditions, specifically in Grimstad, Norway [36]. Nearly all 43 modules suffered from encapsulant defects, namely delamination or discolouration. In Florida, United States, 156 PV modules were inspected after 10 years of deployment and also revealed the same results as [31,36]: all 156 modules exhibited encapsulant delamination failure.

Encapsulant wear-out can result in low optical performance in PV modules, which causes a reduction in the electrical output owing to decreased light absorption and extreme light reflection [89]. The encapsulant discolouration effect begins with a drop in the short-circuit current (I_{SC}). The drop in I_{SC} can be as much as 40%, albeit it is not regarded as a PV failure, as it may not pose a safety hazard [49]. Still, discolouration leads to more severe failures like delamination and corrosion as a result of the release of acetic acid. The released acetic acid in turn is characteristically found responsible for the corrosion of contacts that frequently occurs after the initiation of discolouration failure [90].

With that in context, delamination can cause a substantial decrease in the amount of light absorbed, thereby leading to a significant drop in I_{SC}. Bubble formation is one of the primary triggers of encapsulant delamination; it is formed initially during the lamination process of encapsulation due to a higher localised ratio of released volatile organic compounds [91,92]. The area affected by bubbles in the PV module operates at hotter temperatures and potentially leads to burn marks [93]. A study by Rajput et al. [94] analysed the degradation mechanism of 90 monocrystalline PV modules operated for 22 years in India; it was found that the PV modules affected by more bubbles had more power loss.

Despite ultraviolet radiation occupying a relatively small percentage in the solar spectrum, less than 4%, it is considered a major reason for the degradation of PV encapsulant material [95,96]. Due to its shorter wavelength, ultraviolet radiation possesses greater energy that can gradually degrade the encapsulant, decomposing its polymeric bonds [97]. The UV spectrum is divided into three types: UV-A, UV-B, and UV-C. In deployments, PV modules are not exposed to ultraviolet type-C but ultraviolet type-B radiation. Hence, the latter is regarded as the primary trigger of the degradation mechanism in EVA [98–100].

Even with the implementation of UV-blocking glass, the degradation of EVA remains significant when exposed heavily to UV-B, particularly in conjunction with other stressors such as high temperatures and humidity [61,101]. Consequently, a chemical process is instigated, resulting in the creation of acetic acid and aldehyde, which leads to a gradual darkening of the EVA material from clear to dark brown in severe instances [101,102].

Miller et al. [76] examined five types of encapsulants, exploring the degradation process after exposing them to an artificial ultraviolet source and different combination levels of humidity and temperature. Their experiments revealed that encapsulants had higher degradation rates when they were exposed to lower humidity and higher temperatures, displaying faster yellowing. Experiments for exposing PV encapsulant to ultraviolet sources with stressors were also conducted by Arularasu [103] and showed similar results to Miller et al. [76].

To account for the degree of encapsulant yellowing, a "yellowing-index" terminology, published by the International Organization for Standardization (ISO) [104], is used. Yellowing index is defined as the alteration of polymer colour toward yellow [104]. Nevertheless, Oliveira et al. [105] discovered that early degradation of EVA cannot be spotted as it may start before its colour turns yellow, i.e., the yellowing index has not experienced any modifications. This ambiguity has driven more investigations, for example [59,106,107], to explore the initial stage of EVA degradation. See Figure 5 for examples.

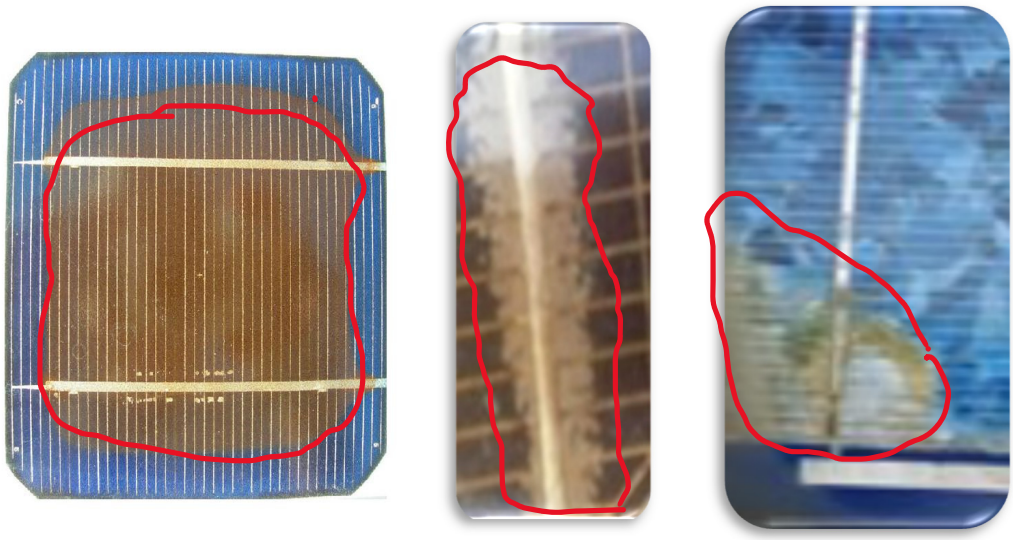

(**a**) (**b**) (**c**)

Figure 5. (**a**) Brown discolouration of PV cell [108]. (**b**) PV module affected by delamination [66]. (**c**) PV module affected by delamination that led to corrosion [109].

The latter might be the one of reasons for Ferrara and Philipp [110] stating there is no distinct correlation between the shift in EVA's colour and the solar cell's electrical performance. However, Rosillo and Alonso-Garcia [111] demonstrated through experimentation that an increase in the yellowness index reduces the major electrical parameter maximum power output. The results of their study are consistent with the well-known research conducted by Pern et al. [112], which examined the electrical performance of solar cells for five different colours of EVA (clear, yellow-brown 1, yellow-brown 2, brown, and dark brown). The researchers concluded that as the EVA colour darkened, there was a gradual decrease in maximum power output, with the greatest reduction observed in the dark brown colour [99].

In addition, Dechthummarong et al. [113] took measurements of PV modules before and after they were mounted for 15 years to ascertain whether the insulation resistance still complied with the IEC 61215 standard [114]. The researchers categorised EVA discolouration into four colours: light yellow, yellow, brown, and dark brown. Their findings revealed

that the modules with light yellow and yellow discolouration exhibited healthier performance with superior efficiency when compared to the brown and dark brown EVA modules. Surprisingly, the insulation resistance of all PV modules met the IEC 61215 standard, even though modules with brown and dark brown discolouration were more vulnerable to failure from corrosion, delamination, and EVA bubble formation. An investigation conducted by Diniz et al. [115] also found that modules with brown discolouration were associated with more severe and safety-related failures, including corrosion.

2.3. Solar Cells

Solar cells are connected in series and then encapsulated, typically with EVA, to provide adhesion between the solar cells and the protective glass. Failure of the solar cell mainly occurs due to the very thin profile of the silicon wafer. These thin wafers are very brittle and are prone to cracking easily during manufacturing or transportation.

Generally, microcracks of the cell cannot be detected by the naked eye. Consequently, they may spread and distribute to other cells in the module [15]. When the cracks prevent more than 8% of the cell from functioning, it may lead to a hotspot [15,116]. The active area of the cracked cell may be forced to operate in reverse bias, eventually causing a hotspot failure. Moreover, cracks are subject to expansion and seeding more cracks, especially under environmental and mechanical stress factors like hot, cold, and windy climate conditions [117–120]. Consequently, they accelerate the ageing process, showing a higher degradation rate [15]. Buerhop et al. [121] reported that PV modules with cracked cells had a greater than 10% power loss after six years of operation when compared to healthy ones. A study by Siruvuri et al. [122] developed a deep learning model based on four attributes—crack type (edge or centre), size, orientation angle (angle in degrees of the crack: horizontal vs. vertical cracks), and ambient temperature—to forecast the impact of crack severity on power loss. The outcome results were analysed and evaluated, revealing that power loss increased with increasing crack size and temperature but decreased with increasing orientation angle. However, with regards to angle orientation, their results contradicted the results of Dhimish et al. [123], where horizontal cracks were more gentle than vertical cracks or so-called parallel to busbar [124].

Conversely, snail track failure can be detected by the naked eye; this failure is so named because it is shaped like a snail's trail. Dolara et al. [125] indicated that most snail track failures are linked to the existence of cracked cells. They also compared four PV modules with a snail track against a healthy one. In their findings, maximum power output dropped in all PV modules with a snail track, one of which had a power loss of 40% of rated power. This reduction in maximum power was caused primarily by a significant reduction in I_{SC}, despite a slight increment in open-circuit voltage (V_{OC}). This association between cracked cells and snail tracks was also stressed in a recent investigation conducted in Indonesia [126]. Duerr et al. [127] found that four degradation mechanisms trigger snail track failures, depending on the combination of the encapsulant materials, and on that basis, snail tracks should be described and categorised under PV failures rather than a single degradation mechanism.

Potential-induced degradation (PID) is another PV failure mode. First observed in Germany in 2005 [128], it degrades PV wafers and leads to the development of hotspots [13,14]. It is formed owing to polarisation differences between the PV module frame and the module's cells. Thus, it mostly occurs in PV plants and farms where PV frames are grounded as a protective technique against fire ignition [129]. If undetected, it may lead to 100% power loss within a few years [56]. A report based in Germany stated that PID failure progresses rapidly with the release of acetic acid due to EVA discolouration [130]. Moreover, in a lab experiment by Pingel et al. [131], the PV module was found unlikely to recover from PID when operated at higher temperatures. With the rise of bifacial PV module deployment in the last decade, Molto et al. [132], reviewed the PID failure displayed in these module types. Although bifacial modules joined the PV market recently, over 30 scientific papers on such failures have been published in the literature. The review analysis of Molto et al. [132]

came up with four classifications of PID failures: PID-s, Na-penetration-PID, PID-p and PID-c. Both PID-s and Na-penetration were caused by the leaning and movement of Na-Na-positive ions to the polarised cells. Involvement of Na^+ ions were also found in PID-c type, which was also classified into three categories, whereas PID-p was related to the deterioration of the PV surface. Recovery of all types was found to be possible either fully or partially via dark storage or ultraviolet lighting, particularly for PID-p, but was found to be irreparable for the PID-c type [132].

Another failure that solar cells might experience is through disconnection of solar cell busbars or ribbons. This type of failure occurs because of a manufacturing defect; it is also driven by excessive heat due to long partial shading and can produce excessive leakage current. When undetected, it increases cell temperature and forms a hotspot [133]. Such failures can be detected by an infrared (IR) camera or by monitoring the output *I*–*V* curve. When this failure occurs, the output power typically decreases by ~35%. With progression, the power will decrease by ~46% [33]. Consequently, the solder bond will become extremely hot, leading to burn marks and discolouration of the EVA encapsulant [134]. In the worst-case scenario, the protective glass will be broken, with visible burn marks on the PV module's backsheet blocking the current path and initiating an electrical arc and fire, causing irreversible damage [15].

Colvin et al. [135] explored interconnection failures depending on cut location in the PV module and irradiance. They investigated cuts in busbars that connect cells in the centre of the PV module and cuts in outer busbars (at the edge). Results showed that outer busbar cuts are more severe and reduce module power output by nearly double compared to cuts in centred busbars. Their findings were justified by the fact that alternative busbars that can carry the captured photocurrents are limited to one when cuts occur at the outer busbar, whereas in inner cuts, there is more than one alternative busbar that can act in place. Majd et al. [136] explored failure immunity in three common interconnection types in PV modules through FEM simulation: the first one is the conventional interconnection known as front-to-back interconnection; the second type is the light-capturing type, which is named due to the recapturing of lost photons via reflection; the third type is the multi-busbar, which uses its rounder shape to reflect the lost light to the cell. Among the three, the multi-busbar type showed 15 per cent higher immunity against ribbon and busbar failures. Examples of various failure types are shown in Figure 6.

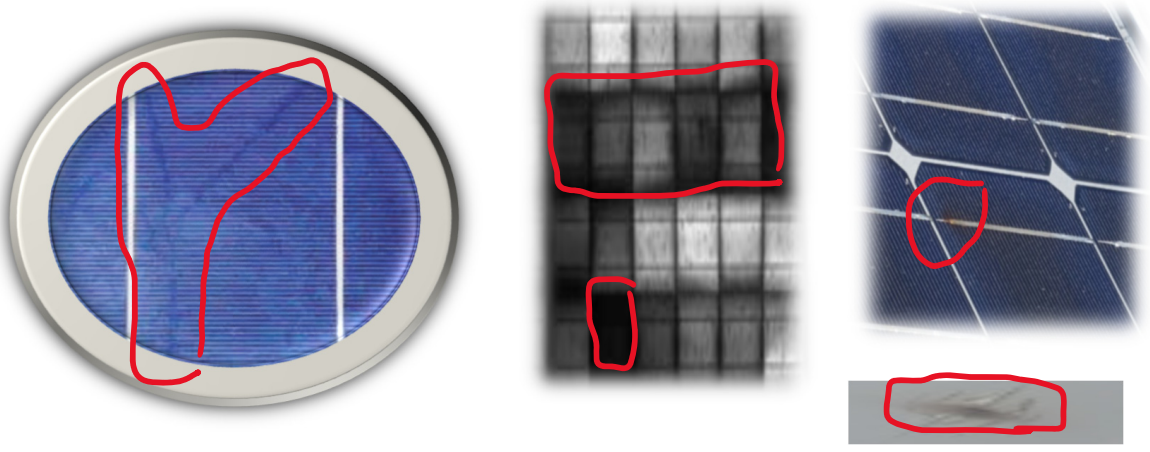

(**a**) (**b**) (**c**)

Figure 6. (**a**) PV module affected by snail track failure [127]. (**b**) PID failure detected by electroluminescence image [137]. (**c**) Hotspot burned the cell solder bonding and exhibited burn marks on the backsheet [138].

Thus, as with most PV failures, early detection is essential to assure a reliable and safe operation of the PV system.

2.4. Backsheet

The backsheet is the last protection layer of the PV module that provides construction support to the PV module. It shields the module's electrical parts from short-circuit failure, ensuring perfect electrical insulation from various environmental stress factors such as water ingress from high relative humidity [139]. Failures and degradation in the backsheet can appear as cracks, discolouration, delamination, bubbles, and burn marks [130].

The major cause of burn mark failures are hotspots, and this may lead the PV module to catch fire. For this purpose, a study conducted by Cancelliere and Liciotti [95] investigated fire reactions with four material arrangements on the basis of a PET (polyethylene terephthalate) backsheet: three layers (PET/PET/primer), four layers (PET/aluminium/PET/primer), three layers (fluoro-coating/PET/EVA), and PET layer with an outside and inside coating. Two backsheets—PET monolayer with an inside and outside coating and the four-layer backsheet (PET/aluminium/PET/primer)—reacted slower to fire and had fewer damaged areas with no or less harm to the EVA encapsulant. However, the monolayer with an inside and outside coating backsheet is favoured over the other as aluminium is electrically conductive and may result in less power production. PET backsheets were also compared for cracking against backsheets made of PP (polypropylene) by Oreski et al. [140]. That comparative study employed an accelerated stress test to explore if PP backsheets have the same immunity as PET backsheets. They found that PP exhibited cracking after the same exposure time as PET, which makes it a reliable substitution for PV backsheets. Further to this, Elfaqih et al. [141] suggested mixing PP backsheets with 5% carbon fibre to provide greater strength and longer reliability against failure. They came up with their proposal after they investigated PP and PPCF (PP supported with carbon fibre) and found that the PPCF backsheet has higher tensile strength.

Investigations of PV module backsheets deployed in outdoor conditions were also conducted by Pascual et al. [142]. In their study, PV modules were deployed in an 8 MW plant. All of them were from the same manufacturer but with two backsheet types: PVF (fluorinated) and polyamide. The PV modules were deployed in 2011 and investigated after six years of operation. Visual inspection revealed that 14% of modules with polyamide backsheets suffered from cracks. Furthermore, polyamide backsheets were susceptible to chalking, which is the decomposition of backsheet material into white powder and is considered a warning sign of abnormal degradation [143]. More than 90% of inspected PV modules with polyamide backsheets degraded by chalking, while none of the PVF backsheets did. The strength of the PVF backsheet might be one of the reasons that has driven research efforts, e.g., [144,145], to search for effective ingredients to be used in accelerated stress tests.

Regarding cracking, Mühleisen [146] developed a solution based on polyurethane paint to be coated at the early onset of backsheet cracking. The coating was examined for nearly two years in outdoor conditions and was also tested under accelerated stress tests. Their results showed a significant reduction in crack progression in coated backsheets compared to uncoated ones. The study of Mühleisen [146] is not the first of its kind, as Beaucarne et al. [147] also fabricated a coated solution of a flowable silicone sealant that can act in place to avoid early replacement of PV modules. They applied the solution on PV modules operated for less than 8 years with heavy backsheet cracks. These modules included four types of backsheet: co-extruded polyamide, PVF, PVDF, and PET. The cracked backsheet modules were tested for insulation resistance and none of them passed the required standard level. After applying the coating, all of them were restored to a healthy level of insulation resistance even after applying accelerated stress tests for a thousand hours. Examples of backsheet issues are shown in Figure 7.

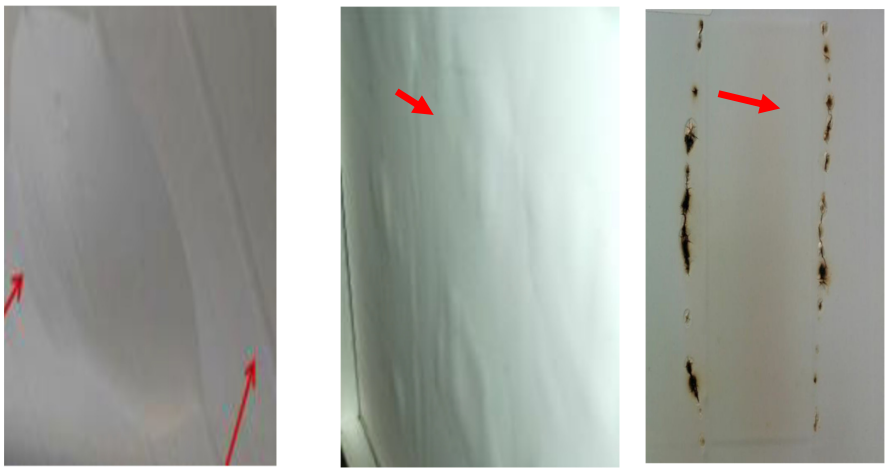

(**a**) (**b**) (**c**)

Figure 7. (**a**) Backsheet bubbles [130]. (**b**) Backsheet delamination [130]. (**c**) Burn marks caused by a hotspot in the backsheet [138].

2.5. Junction Box and Bypass Diodes

A junction box (J-box) is attached to the PV module through adhesive material to regulate and provide a safe flow of the collected photocurrents into the PV module [148]. To guarantee the correct flow path of the current, bypass diodes are also installed inside the J-box in different configurations: overlap and non-overlap [149]. Failures in the J-box are mainly caused by low wiring quality, blown bypass diodes, corrosion, and poor bonding to the PV module (delamination), caused primarily by high humidity [87]. Failure of the J-box may result in zero output of electricity, as was found by Bakir [150] in a recent assessment of a 23 MW PV plant mounted in Turkey. As of the writing of this paper, many studies, e.g., [151,152], have come up with novel techniques to monitor and protect J-boxes from failures. Most J-box failures allow for the ingress of water vapor, causing serious safety issues, such as initiating an electrical arc or causing hotspots [15]. Ong et al. [153] listed J-box failures among the root causes of fire ignition in PV modules. Han et al. [21] investigated the condition of 177 monocrystalline PV modules that operated for 22 years in a humid climate with an average temperature of 27.5 °C. Most of the junction boxes of the modules had been seriously damaged and needed replacing.

Furthermore, junction boxes can degrade at a faster rate when exposed to large variations in ambient temperature during the year. Daher et al. [154] evaluated the reliability of a 9-year PV system (270 modules) installed off-grid that was expected to produce 62 kW in Ali Adde town, Djibouti. The PV system was exposed to the town's high temperatures with dramatic variation from winter (average temperature is 26.7 °C) to summer with an average of 38 °C. Out of 270 modules, 39% were diagnosed with adhesive junction box failure.

On the other hand, cold climates with high relative humidity like that of Grimstad, Norway, led to the corrosion of junction boxes [36]. J-boxes and metal parts of PV modules operating in so-called floatovoltaics structures, such as PV systems deployed on the water in a floating construction, are also at higher risk of corrosion [155]. This urged Ghosh [156] to recommend that J-boxes should have a protection rating of IP67 when attached to PV modules mounted in a water-based environment. Unsurprisingly, dust has also been found to corrode the PV module's junction box. Tabet et al. [157] inspected a module operating in a dusty environment for six years, finding that the J-box failed because of corrosion. This is in agreement with the finding of Lin and Zhan [158] that water-dissolvable salts represent more than 59% of dust composition, in which, whenever stuck to metal, they react and cause corrosion, primarily in humid environments.

Several PV failures were found to form hotspots, making it necessary to protect the PV module. One means of protection is to use a bypass diode, although it has been criticised

for being neither safe nor effective [72,159,160]. The existence of a bypass diode enables the current to flow over the defective solar cells, thereby protecting the PV module from thermal increases and hotspots. This is one of the main explanations why some PV manufacturers, such as AE-Solar, a German PV manufacturer, attach a bypass diode to each PV cell [161]. One of the recurrent reasons for blown bypass diodes is the increase in their temperature due to long-term shading [162,163]. Also, it was indicated by Bansal et al. [87] that those bypass diodes that were exposed to overirradiance, in particular over 1400 Wm^{-2}, are expected to be blown due to excessive currents.

Failure to detect poor bypass diodes may lead to serious safety issues [163,164]. Since bypass diodes are used to avoid PV failures that lead to hotspotting, whenever they fail, the module loses its means of protection, becomes vulnerable, and, in the worst scenario, initiates fire [41,165]. Bakir [166] used an infrared imaging detection technique where he attached thermal cameras to a drone to be flown over three solar plants that ranged between 2 and 3.5 MW. One of the plants had three PV modules with failed bypass diodes and as a result, their operating temperature increased by an average of 19.7 C. It was shown by Ghosh et al. [167] that the operating temperature of PV cells undergoing shading failure decreases by nearly 50% when bypass diodes are functioning. Their experimental study aimed to explore if total cross-tied (TCT) array configurations were effective in preventing hotspots by allowing the bypass diodes to respond promptly in cases of shading. The study also showed that bypass diodes were only functioning if more than one cell was affected by shading and, therefore, further investigations are required to pinpoint the optimal configuration of PV arrays that is able to activate bypass diodes even in the case of one shaded cell, such as situations of fouling by bird droppings. Examples of these failures are shown in Figure 8.

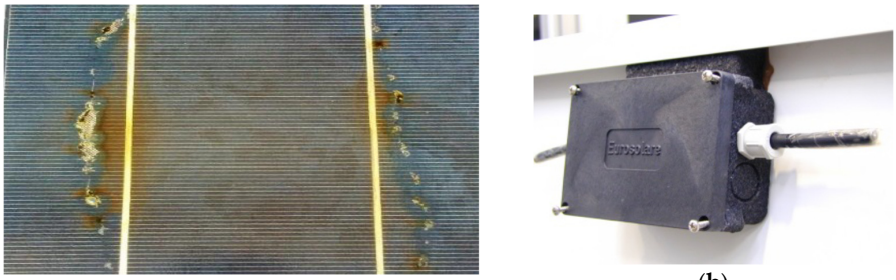

(**a**) (**b**)

Figure 8. (**a**) Failed bypass diodes leading to hotspots [138]. (**b**) Poor bonding of J-box [137].

To conclude this Section 2, PV failures can be classified based on the components affected. The same PV failure mechanism can be seen or experienced in more than one component due to the similarity of the materials; e.g., EVA is present in encapsulants and also in backsheets. Furthermore, EVA defects are usually considered an early sign of PV module degradation and failure as EVA, alongside PV glass, represents the first defence line against weather stressors. Unlike snail tracks in PV cells, corrosion is another failure mechanism that can attack more than one component, such as solar cell solders, bypasses, and junction boxes, especially in humid environments.

The hotspot failure mechanism is considered the most severe failure and leads to catastrophic consequences. It deteriorates all PV module components if undetected, and a PV module affected by an elevated level of hotspots cannot reverse the degradation and often requires replacement. Thus, identifying the initial stages of PV degradation can prevent potential hazards through proactive maintenance. Sometimes, it is even more effective to substitute a PV module that displays the early onset of deterioration as it will guarantee all deployed modules in PV plants continue generating the healthier (expected) power, regardless if their condition complies with the IEC 61215 standard [114]. Table 2 lists the PV failures reported in investigational studies within the last two years, classifying them on a PV component basis.

Table 2. PV failures reported in investigational studies within the last two years.

Component Impacted	Defect (Failure)	Type of PV (Poly-Si, Mono-Si)	Operational Time (Year)	Failure Detail	Country	Ref.
Protective glass	Breakage	Mono-Si	16 and 13	Two occurrences owing to poor transportation and vandalism.	Indonesia	[126]
		Poly-Si	20	None of the 43 PV modules affected by breakage of glass.	Norway	[36,37]
		Not Stated	Not Stated	52 modules affected in three PV plants ranging from 2 to 3 MW.	Turkey	[166]
		Poly-Si	6	Rare occurrences of glass breakage accompanied by cracked cells and dark EVA discolouration. Potential causes: hotspot, harsh weather (high wind speed and dust), and incorrect installation.	India	[29]
		Poly-Si	10	Less than 1% out of 2078 investigated modules. Possible causes: wind, hotspots, and handling.	India	[30]
EVA	Discolouration	Poly-Si	5 [(a)], 9 [(b)], 5 [(c)], and 10 [(d)]	Dark [(a)], light yellow [(b)], dark [(c)], and brown [(d)].	Ghana	[31]
		Mono-Si	15 [(a)] and 5 [(b)]	Light yellow [(a)] and light brown [(b)].		
		Both types	16 and 13	Not specified.	Indonesia	[126]
		Poly-Si	20	Nearly all investigated (43 PV modules) affected.	Norway	[36,37]
		Mono-Si	10	2 out of 156 PV modules displayed brown discolouration.	U.S.	[32]
		Both types	11	Prevalent among all PV modules, resulting in up to 18% reduction in short-circuit current and potentially brown discolouration [168].	Algeria	[33]
		Poly-Si	6	Rare occurrences of light discolouration in 10 MW PV plant.	India	[29]
		Mono-Si	11	Brown discolouration was detected in 10% of the PV modules.	Algeria	[34]
		Poly-Si	10	Roughly 14% of the 2078 investigated modules were affected by yellow and brown discolouration.	India	[30]

Table 2. *Cont.*

Component Impacted	Defect (Failure)	Type of PV (Poly-Si, Mono-Si)	Operational Time (Year)	Failure Detail	Country	Ref.
EVA	Delamination	Both types	8y-poly and 15y-mono	Rare occurrence with fewer than 4 modules impacted out of 104 of all types.	Ghana	[31]
			16 and 13	Several occurrences, especially in the 12-year PV system.	Indonesia	[126]
		Poly-Si	10	Dominant among the 43 PV modules, mainly at the cell edge.	Norway	[36,37]
		Both types	10	Rare occurrences, only 11 out of 2078 investigated modules; potential cause was weather condition.	India	[30]
		Mono-Si	10	All investigated (156) PV modules were influenced near the busbar; root cause expected to be heat resulting from busbar resistance.	U.S.	[32]
		Both types	11	Potential cause: desert weather.	Algeria	[33]
		Mono-Si	11	25% of modules experienced delamination, some at the centres and others at the edges.	Algeria	[34]
Solar cells	Cracks	Mono-Si	5 and 15 years	Extremely rare: only two of 104 modules were affected. Possible cause was unknown.	Ghana	[31]
		Poly-Si	20	Prevalent among the 43 PV modules, predominantly at the cell edge.	Norway	[36,37]
		Mono-Si	10	Few cracks were detected in PV modules inspected by EL imaging.	U.S.	[32]
		Poly-Si	14	Results from EL imaging showed that 9 out of 10 modules have crack cells.	Germany	[35]
	Corrosion	Both types	20	12 out of 104 modules were affected.	Ghana	[31]
	Snail Track	Both types	5	Rare occurrence, with fewer than 4 modules impacted out of 104 of both types. Claimed to be caused by manufacturing process.	Ghana	[31]
			16 and 13	Several occurrences, especially in the 12-year PV system.	Indonesia	[126]

Table 2. *Cont.*

Component Impacted	Defect (Failure)	Type of PV (Poly-Si, Mono-Si)	Operational Time (Year)	Failure Detail	Country	Ref.
Solar cells	Snail Track	Mono-Si	11	2 out of 20 modules suffered from snail tracks, one of which was inked with cracked cells.	Algeria	[34]
		Mono-Si	10	30 out of 156 PV modules displayed snail track.	U.S.	[32]
		Poly-Si	10	Roughly 1.5% of 2078 investigated modules were affected, with snail track often linked with cracked cells.	India	[30]
	PID	Poly-Si	20	One investigated by EL imaging; cell crack seems to be the cause of PID.	Norway	[36,37]
	Hotspot	Poly-Si	20	One investigated by IR imaging; suspected to derive from cracks.		
		Mono-Si	10	10 modules suffered from hotspots and displayed burn marks on the backsheet.	U.S.	[32]
		Not stated	Not stated	One module was detected in a 2.7 MW PV plant.	Turkey	[166]
		Poly-Si	6	Suspicion in one module of one module. Potential cause: mismatch.	India	[29]
		Poly-Si	14	3 out of 10 modules showed hotspotting, detected by IR.	Germany	[35]
		Poly-Si	10	Detected in 10 out of 2078 investigated modules.	India	[30]
Backsheet	Chalking	Mono-Si	11	1 out of 20 modules.	Algeria	[34]
	Discolouration	Both types	8	Nearly 14 modules were affected out of 104 of both types, specifically those lacking mounting support.	Ghana	[31,37]
		Poly-Si	10	11 out of 2078 investigated modules failed with burning and cracks. Possible causes are hotspots and failed J-boxes.	India	[30]
	Delamination	Mono-Si	10	29 out of 156 PV modules suffered from backsheet delamination failures like bubbles.	U.S.	[32]

Table 2. *Cont.*

Component Impacted	Defect (Failure)	Type of PV (Poly-Si, Mono-Si)	Operational Time (Year)	Failure Detail	Country	Ref.
J-Box	Corrosion	Mono-Si	16	Several occurrences.	Indonesia	[126]
	Delamination	Both types	13	Poor installation was potentially the cause.	Indonesia	[126]
		Mono-Si	11	1 module had a detached J-box.	Algeria	[34]
	Burning	Poly-Si	10	Only detected in 2 out of the 2078 investigated modules.	India	[30]
	Bypass diodes	Not stated	Not stated	Detected in 8 modules in a 2.7 MW PV plant.	Turkey	[166]

(a), (b), (c), (d): These refer to the operating times given in the preceding column and using the same superscripts.

3. Classification of Crystalline Photovoltaic Module Failures

Failures can be classified into different criteria based on severity, location of the failure, and occurrence time (whether it occurs early after installation or in the last years of warranty). Kuitche et al. [169] classified failure types based on severity level; the severity of failure was mathematically estimated using Equation (1) [169].

$$RPN = S \times O \times D \quad (1)$$

where RPN is defined as risk priority number used as a rating guideline.

S is the severity rating and it is rated from 1 to 10, where 1 refers to no apparent defect and 10 indicates no operation.

O is failure occurrence and it is rated from 1 to 5, where 1 indicates failure is less likely to occur and 5 indicates a frequent occurrence of at least once per month.

D is the detection of the failure and is rated from 1 to 10. One indicates the failure will be easily detected, and ten means it is less likely to be spotted.

Similarly, Jordan et al. [16] adopted Equation (1) to extract a classification method based on severity. They ranked the severity from 1 to 10, where 1 indicates there is no effect on the performance of the PV module and 10 points to a severe impact on performance accompanied by a safety hazard. Within their classification, hotspot failure ranked 10, and a minor delamination failure rated 1. Tsanakas et al. [56] classified PV failure differently based on optical and electrical shortages. Failures that can be visually identified were categorised as optical failures and those that require measurements of their parameters were categorised as electrical failures. On the other hand, Kontges et al. [15] classified PV failures into three categories based on the expected time of occurrence in the PV lifecycle: infant-life, mid-life, and wear-out failures. Infant-life failures are the ones that appear in the early life of PV operation. Mid-life failures arise after eight years of operation, whereas wear-out failures are failures that emerge just before the end of the module's expected lifetime. A recent review by Hong and Pula [170] classified PV failures based on connections: whether the failure represents a ground or line-to-line fault. A list of PV failure classifications is summarised in Table 3.

Table 3. Photovoltaic failure list classified by three different reviews.

Photovoltaic Failure	**Classified by Jordan et al. [16]. Classification Categories: Severity 1 to 10**	**Classified by Tsanakas et al. [56]. Classification Categories: (a) Optical; (b) Electrical; (c) Not Classified.**	**Classified by Köntges et al. [15]. Classification Categories: (a) Infant-Life; (b) Mid-Life; (c) Wear-Out.**	**Classified by Hong and Pula [170]. Classification Categories: (a) Mismatch; (b) Ground; (c) Line; (d) Arc; (e) Other.**
Hotspot	10	Electrical	Not Classified	Other
Encapsulant Delamination	Minor Delamination: 1 Major Delamination: 5	Optical	Mid-Life	Mismatch
Encapsulant Discolouration	3	Optical	Mid-Life	Mismatch
Solder Bonding	8	Electrical	Wear-Out	Ground and Arc
Glass Breakage	5	Optical	Infant-Life	Other
Cracked Cell	5	Electrical	Mid-Life	Other
Bypass-Diode	5	Not Classified	Mid-Life	Other
Junction Box	5	Electrical	Infant-Life	Arc

4. Effect of Environmental Stress Factors on PV Degradation

Each manufactured component in the industry has a tolerance rating in relation to environmental stress factors, which include temperature, humidity, wind, ultraviolet light, snow, and dust. PV module components are no exception in this regard [171]. Harsh weather, including, but not limited to, high and low temperatures, high relative humidity, dust storms, snowstorms, and high UV index, are aspects of environmental stress factors that reduce the PV module's efficacy and trigger degradation early in its lifespan. For instance, increases in ambient temperature above 25 °C reduces the power production of PV modules [172,173].

Such failures as potential induced degradation, encapsulant discolouration, and delamination were listed to be triggered by high ambient temperature by Köntges et al. [15]. Humidity triggers the adhesion of the module's backsheet and raises safety concerns in PV systems when water vapor penetrates the module's conductive parts and junction box [15,21]. Humidity makes a significant contribution to the corrosion of the J-box as it first deteriorates the bond force of cohesive material and secondly allows water to breach and react with metal [174]. Dust particles and snow were reported to cause shading failures and reduce power output significantly [3]. Both extreme cold and hot climates were found to increase the degradation rate of PV modules as well as increase the expansion of cracked cells [30,137,175].

Santhakumari and Sagar [174] reviewed the literature focusing on failures related to weather conditions and their contribution to the degradation of photovoltaic system components, including batteries, cables, and inverters. Their review concluded that high ambient temperature, relative humidity, dust, sandstorms, and hailstorms highly trigger PV failures, causing optical and electrical losses. These environmental stress factors were found to trigger encapsulant degradation, corrosion, and glass breakage. The review [174] also addressed some of the experiments that have been conducted to tackle harsh environmental stress factors. For instance, sprinkling water on PV panels was an efficient technique to reduce the operating temperature of the PV module. The kinds of failure classified by Santhakumari and Sagar [174] as triggered by high relative humidity were also found by Chandel et al. [66] in monocrystalline PV modules deployed in a humid environment in India, with a nearly doubled degradation rate of 1.4%.

Dust accumulation is another environmental stress factor that decreases power output by limiting light transmission to the PV surface. It occurs in locations where dust storms are common, such as parts of the Middle East and Africa. Dust particles either scatter light in the atmosphere or accumulate on the PV module surface [176]. When dust scatters in the atmosphere, it reduces the irradiation reaching the Earth's surface and converts it to diffuse irradiance, slightly reducing the overall power. In contrast, dust accumulation on the PV surface directly impacts power output and is thus a more obvious effect warranting further investigation. It has motivated researchers who live in harsh weather environments to conduct more studies during dust storms [177], while others have set up lab experiments to investigate different dust particle properties on PV modules [178,179].

Saidan et al. [177] compared electrical parameters between PV modules at different periods of dust accumulation. They concluded that the reduction in short-circuit current and power output became greater after longer periods of dust accumulation. That is, I_{SC} was decreased by fourfold when dust accumulated for one month compared to one day. This is in agreement with Said and Walwil [180], who investigated dust accumulation on PV modules deployed in Dharan, Saudi Arabia; I_{SC} was more reduced in a more extended time of dust accumulation.

Many factors need to be considered to address PV dust and snow accumulation; tilt angle is one of them. Sayigh et al. [181] experimented with PV modules operated in the field for 38 days at different tilt angles ranging between 0° and 60°. They found that dust accumulation increased dramatically when the tilt angle decreased, causing a reduction in the PV transmittance. This was also tested and confirmed by Said and Walwil [180]. Both Elminir et al. [182] and Said and Walwil [180] showed that dust accumulation increased

fivefold at a tilt angle of 0° compared to a tilt angle of 90°. Properties of dust particles, weather conditions, and dust adhesion force also play a vital role in tackling the dust accumulation problem. For example, adhesion force for larger dust particles was higher than for smaller ones [179,180].

A lab experiment conducted by Mehmood et al. [178] identified the material components of the dust particles found in Dhahran, Saudi Arabia, and their mud characteristics when they reacted with moisture on two PV surfaces: glass and polycarbonate. The dust particles collected from the PV module's surface were mixed with different concentrations of deionised water, applied to the glass and polycarbonate, and then dried for two days. Their results showed that the glass's transmittance was reduced by 9% more than that of the polycarbonate.

It is essential to assess the weather conditions for targeted geographical locations when installing a PV system, studying the risks and economic feasibility of extra application of immune material against existing weather stressors. Some weather stressors, like high UV index and humidity, require advanced materials to be overcome, while others may only require continuous monitoring, such as regular cleaning of dust and snow. Hence, early planning and assessment ensure a reliable operation of the PV system, as well as reduce the risk of lost revenue for PV operators by ensuring maximal power generation. For instance, allowing a PV surface to remain unclean in a dusty environment was reported to cause a decrease in power generation by 18% in just one month of dust accumulation [177]. Table 4 lists some recent studies that highlighted weather conditions' effect on PV.

Table 4. PV studies that highlighted weather conditions within the last two years.

Weather Condition	Weather Highlight	Failure Modes Detected or Explored and Component Affected	Type of PV (Poly-Si, Mono-Si)	Lifetime (Years)	Country	Ref.
Subtropical climate with moderate humidity level and high temperature.	Hot	Glass breakage, EVA discolouration, soiling, cracked cell, hotspot.	Poly-Si	6	India	[29]
Semi-desert climate, considerably hot and dry weather.	Hot	Glass breakage, EVA discolouration, soiling, EVA delamination, cracked cell, snail track, metal corrosion, backsheet cracks and burns.	Poly-Si	10	India	[30]
Dry equatorial climate. The average temperature is between 28 °C and 30 °C and the average humidity is between 60% and 75%.	Dry and hot	EVA discolouration, metal corrosion, backsheet defects.	Mono-Si	Between 0 to 5	Ghana	[31]
Wet semi-equatorial climate. The average temperature ranges between 26 °C and 30 °C and the average humidity is between 70% and 80%.	Hot and humid	EVA discolouration, EVA delamination, metal corrosion, backsheet defects.	Poly-Si	Between 6 and 10.		

Table 4. *Cont.*

Weather Condition	Weather Highlight	Failure Modes Detected or Explored and Component Affected	Type of PV (Poly-Si, Mono-Si)	Lifetime (Years)	Country	Ref.
Desert climate hot and dry with moderate to high relative humidity throughout the year.	Dust	Experimental study to address dust effect. Soiling reduced power production by 9% within 30 days.	Mono-Si	Not stated	Oman	[183]
Dry, hot in the summer and moderate temperature with frequent rainfall in the winter.	Dust	PV modules were kept for 6 months for soiling evaluation, result showed 20% power loss despite rainy days in 2 months.	Mono-Si	Not stated	Iran	[184]
Dry, hot in the summer and moderate temperature in the winter.	Dust	PV modules were kept for 6 months for soiling evaluation, an average of 18% of power loss was recorded.	Mono-Si	Not stated	Iraq	[185]
Cold, frequently accompanied by snowstorms.	Cold and snowing	Analysis model to forecast PV production expected 80% power loss if the snow thickness is 60 mm.	Not stated	Not stated	China	[186]
One city has dry and hot weather, whereas the other has lower temperatures.	Hot	Comparison between two PV systems installed in two cities. The one installed in the Mediterranean climate is superior, despite the high humidity level.	Both	Not stated	Morocco	[187]
Hot accompanied by high relative humidity up to 85%.	Hot and humid	EVA discolouration and delamination, snail track, metal corrosion, backsheet cracks and burns, hotspot.	Mono-Si	10	U.S.	[32]
Dry and hot climate, with frequent sandstorms, located in the desert.	Dry and hot	EVA discolouration and delamination, metal corrosion.	Both	11	Algeria	[33]
Hot with a high relative humidity range; average is 67%.	Hot and humid	EVA discolouration and delamination, snail track, metal corrosion, soiling, backsheet chalking, J-box delamination.	Mono-Si	11	Algeria	[34]

Table 4. *Cont.*

Weather Condition	Weather Highlight	Failure Modes Detected or Explored and Component Affected	Type of PV (Poly-Si, Mono-Si)	Lifetime (Years)	Country	Ref.
Moderate climate with considerably high relative humidity which can reach 83% in the winter months.	Humid	EVA discolouration and delamination, cracked cell, metal and bypass corrosion, hotspot, PID.	Poly-Si	14	Germany	[35]
Cold and humid; average temperature range between −6.7 °C and 21 °C; average humidity range between 30% and 99%.	Cold	Glass breakage, EVA discolouration and delamination, cracked cell, metal corrosion, hotspot.	Poly-Si	10	Norway	[36,37]

5. Detection Methods for Failures in PV Modules

Depending on the connection type of the PV system, whether it is grid-connected or standalone, failures occur on two different sides of the connection: DC and AC. They often occur on the DC side when the system is standalone, whereas they may exist on the AC side when connected to the grid. Distinguishing them can be achieved by monitoring the system's power output; it reduces and rarely leads to a blackout in DC failure but causes a total blackout when a failure occurs on the AC side [17].

Madeti and Singh [17] reviewed the literature and classified all failure detection techniques into two groups: (a) fault detection based on the ground, which involves monitoring sensors, and (b) fault detection based on a space monitoring system. The latter group is cost-effective owing to the lack of instrumental sensors, but depending on weather conditions, its accuracy can be reduced dramatically. The sensors employed in ground-based techniques are set to observe major electrical parameters, such as current, voltage, and power. These parameters vary based on the PV system's connection type; for instance, grid impedance exists in grid-connected systems, but not in standalone systems [17].

Each type of PV failure requires a different tactic to be detected. For example, detection tactics employed in optical failures are different from those employed in electrical failures. Optical failures may be seen by the naked eye, whereas electrical losses require instruments to monitor, store data, and perform analyses. Furthermore, detection techniques for failures on the AC side, e.g., failure of PV converter and power blackout of the grid, are utterly different from those on the DC side [17]. This review will briefly examine the failure detection techniques proposed for the DC side (PV module components).

According to Pillai and Rajasekar [18], for a detection technique to be effective, it should meet the following criteria: (1) able to detect failures without interfering with power or causing blackout, (2) able to pinpoint the failure, (3) cost-effective and flexible, (4) simple in structure, and (5) can be applied to a variety of PV systems. Madeti and Singh [17] classified failure detection techniques on the DC side into six categories: electrical characterisation, infrared imaging, visual inspection, ultrasonic inspection, electroluminescent imaging, and lock-in thermography. A similar classification was presented by Santhakumari and Sagar [174], but with fewer details and a different terminology; e.g., electrical characterisation was referred to as indoor testing using a solar simulator. Twelve detection techniques were listed under electrical characterisation in Madeti and Singh [17]; five of them were reviewed in more detail by Mellit et al. [188]. Those five techniques were signal and processing, *I–V* characteristic analysis, power loss analysis, voltage and current monitoring, and machine learning detection techniques.

5.1. Visual Inspection

The first step to detect PV failures is to view the PV modules from different angles. Visualising techniques are demonstrated and reviewed by the international standard IEC 61215 [189]. The standard considers broken, cracked, and misaligned module surfaces as well as bubbles of the encapsulant as significant defects. Failures such as delamination, mild discolouration, corrosion, J-box failure, and shading could be visualised by the naked eye without employing other detection techniques [87,188]. Furthermore, some researchers, e.g., [150,190], proposed the use of drones with installed cameras to visualise PV plants more effectively.

5.2. Infrared Imaging

Infrared imaging is a detection technique based on the solar cell's reversed biased circulating current in a PV module [191]. In the case of failure, the solar cell dissipates heat which an infrared camera can detect, see Figure 9. Hotspots, as well as microcrack failures, sometimes cannot be seen by the human eye. However, they may be caught by infrared imaging. Predicting failure before it takes place is a major advantage of this technique. On the other hand, one drawback is expensive staffing costs [18]. The working principle is usually started by storing images of a healthy PV module to compare them to a faulty module when needed. This technique can detect hotspots, breakage of solar cells, disconnection, and PID failures [87].

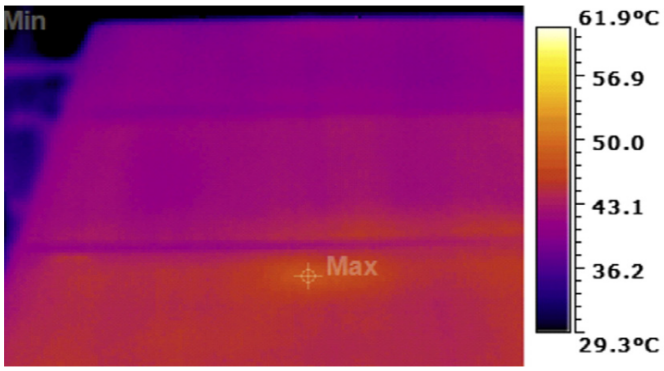

Figure 9. Infrared imaging to discover high-temperature cells in a PV module [18].

5.3. Electroluminescence Imaging

This technique is used to detect a potential cracked cell by pinpointing the low contact area of a PV module [192]. The working principle of this technique is to look into the recombination losses (shunt defects) created by a current injected into the solar cell's metallic contact [193–195]. In addition to detecting cracked cells, snail tracks and PID failures can also be seen using EL imaging [87], see Figure 10 for examples. The lock-in thermography detection technique has nearly the same working principle as EL but was found to be superior and more sensitive in detecting failures [122].

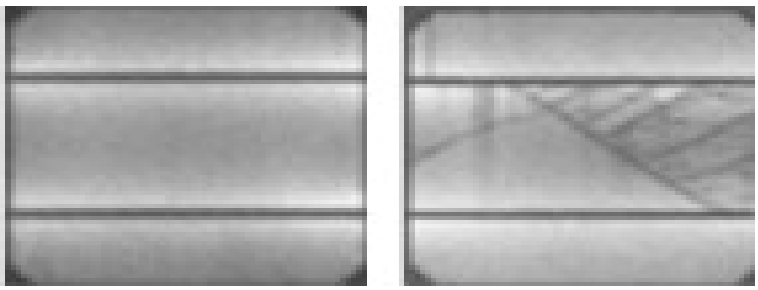

(**a**) (**b**)

Figure 10. (**a**) EL imaging of a healthy monocrystalline solar cell. (**b**) EL imaging of a cracked monocrystalline solar cell [196].

5.4. Ultrasonic Inspection

The ultrasonic inspection detection technique compares the frequency signals of a healthy and a faulty cell obtained by an ultrasonic transducer [197–199]. Resonance frequency tends to decrease when detecting a defective cell [198,200], see Figure 11 for example. The ultrasonic technique is mainly used to detect cracked cells in a PV module. An advantage of this method is that it infers the severity level of the cell crack based on the range of the frequency's bandwidth [198].

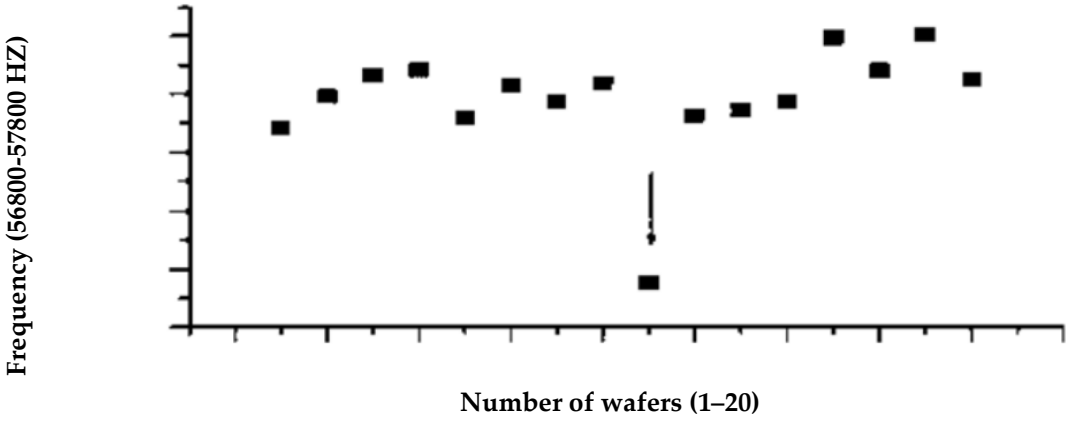

Figure 11. Ultrasonic inspection of several cell wafers showing cell no. 11 has an abnormal reduction in frequency, indicating a crack failure [197].

5.5. Electrical Characterisation

Electrical characterisation has been claimed to be the most common detection technique for PV failures [201]. This detection technique focuses on monitoring and spotting any changes in the PV system's electrical parameters. It was reviewed by Mellit et al. [188] and referred to as a signal-processing approach that involves protection devices such as over-current protection devices. Pillai and Rajasekar critically reviewed protection devices [18], explaining the limitations and drawbacks of detecting a failure instantly, particularly under low irradiance, which may lead to serious safety issues and catastrophic failure. For instance, a delayed response from over-current protection devices during a PV failure leads to an electric arc or fire [188].

I–V curves, power losses, and PV module temperature can all be used to detect PV failures. For instance, if the temperature of the PV module increases due to a hotspot failure, sensors can be put in place to detect abnormal increases [202], and further, insulation monitoring devices can evaluate the resistance between the current-carrying conductor and the ground to detect ground failure [203]. Fuses are able to calculate the residual system's current [204].

One technique of using residuals to detect failures requires the simulation of a healthy PV module to obtain the maximum voltage (V_m), maximum current (I_m), and power values and then compare these values with the actual measured data. Residuals (the difference between the simulation and the experimental values) indicate the existence of a PV failure. Depending on the residual extent, the type of failure can be predicted [205,206]. Harrou et al. [206] used this method as an indicator of abnormal changes in a PV system. However, they concluded the monitored parameters were insufficient to detect extreme degradation and partial shading failures.Garoudja et al. [205] used the residual technique and reached the same result as Harrou et al. [206], predominantly for shading failures. Thus, it is more effective to include other *I–V* parameters as an indicator such as short-circuit current and fill factor.

One obstacle preventing the accurate detection of PV failures is obtaining noisy data from measurements. Harrou et al. [206] focused on detecting four types of PV failures on the DC side: open circuit, short circuit, partial shading, and degradation failures. In order to detect those failures accurately, they used a wavelet-based multiscale tool to separate the

noisy measurement data. Garoudja et al. [205] also concluded that using wavelet-based multiscale anti-noise techniques increased the accuracy of PV failure detection. Noisy data seem to be an obstacle in Ali et al. [207], who ended up suggesting to separate them using noise separation devices or working out efficient ways for noise separation. However, with advanced technologies at present, artificial intelligence (machine and deep learning) in particular, noisy data have been tackled in many recent studies, e.g., [208,209]; that is, the accuracy of PV failure detection was robust even with the presence of noisy data.

5.5.1. Detection Techniques Using *I–V* Curve Parameters

The *I–V* curve, see Figure 12, shows the output combinations between voltages and currents, delivering the values of major parameters: short-circuit current, open-circuit voltage, maximum power output, and fill factor. Modelling of healthy or expected *I–V* curves and power output via engineering modelling programs is also classified under electrical characterisation and was referred to as "model-based difference measurements" by Pillai and Rajasekar [18]. One of the reasons for simulating the *I–V* curve, instead of obtaining it experimentally, is the risk associated with performing faulty operation scenarios in a real PV plant, which may get out of control [210].

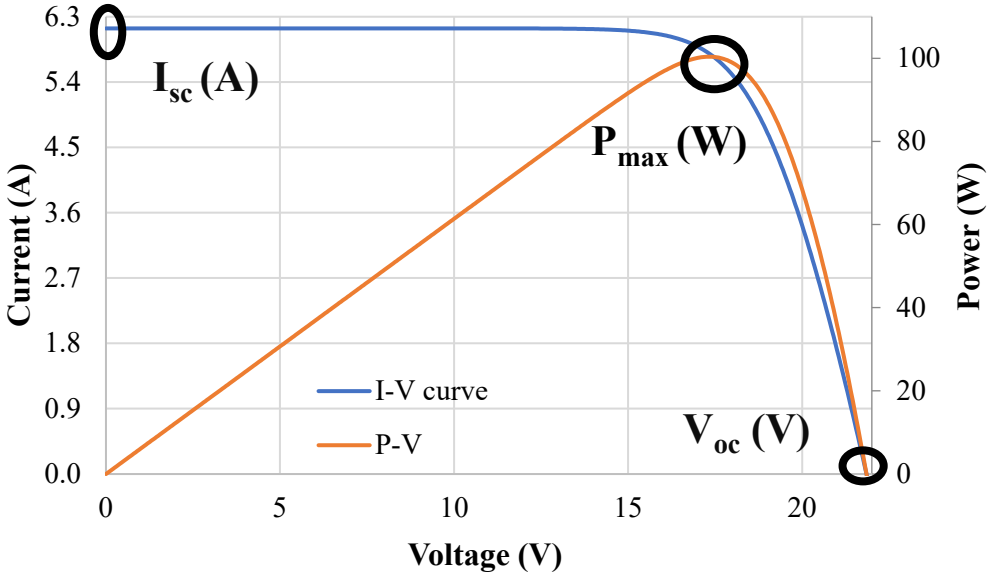

Figure 12. Current–voltage and power–voltage curves display the major parameters of a solar cell; I_{sc}, current at zero volts; V_{OC}, voltage at zero amps; and P_{max}, maximum power output. The circles show the location of short circuit current, open circuit voltage and maximum power point.

Chen et al. [211] investigated four failure modes and recorded their impacts on the *I–V* curve. Short-circuit failure was found to decrease both P_{max} and V_{OC}. Degradation failure could be observed when a reduction in the *I–V* slope accompanied a gradual decrease in P_{max}. I_{SC} was decreased in open-circuit failure. In case of partial shading failures, the *I–V* curve was distorted, forming multiple P_{max} points; one before shading and one after shading. Ali et al. [207] fabricated three shading scenarios on a PV string that contained three polycrystalline modules; firstly, one-third of two modules were shaded; secondly, three cells in each module were shaded; and lastly, half of the cells in each module were shaded. As a result, *I–V* curves were distorted, and V_{OC} decreased in all three scenarios. The greatest value was seen in the third scenario, with a 68% reduction.

Köntges et al. [15] agreed with Ali et al. [207] that shading failures distort the *I–V* curve, creating multiple P_{max} points. They also listed the effect of various PV failures on the *I–V* curve; I_{SC} is affected mainly by optical failures and losses of transparency, EVA discolouration, glass breakage and shattering, and EVA delamination. It is also affected by disconnected soldering of the cells, PID, and cracked cells in the PV module. On the

other hand, V_{OC} is affected by defective bypass diodes, PID, and disconnected soldering of the cells. The fill factor is affected by delamination, corrosion, and cracked cells. All PV failures were found to reduce P_{max}, except for bypass defects.

The awareness of the electrical characterisation's boundaries assists in training supervised machine learning algorithms by looking for deviations from their previous relationships to detect PV failure and degradation. Chine et al. [212] implemented artificial neural networks (ANN) to detect eight types of faults related to shading caused by snow and soiling. A probabilistic neural network (PNN) algorithm was implemented to predict and classify three failure mechanisms by Garoudja et al. [210] and was found to be superior and more efficient than ANN, even in the presence of noise. The substantial number of published studies that proposed or developed artificial intelligent models to detect PV failures demanded a review to arrange, compare, and classify them. Researchers in recent years were aware of this gap and many reviews were conducted as a result, e.g., [170,213–217].

5.5.2. Detection of Degradations and Failures Using Shunt and Series Resistance

Modelling of the *I*–*V* curve's major parameters, e.g., short-circuit current and open-circuit voltage, via mathematical equations assists in extracting the values of other key parameters [218,219], namely series resistance and shunt resistance. As most PV failure and degradation modes will severely impact these parameters, quantifying them will significantly enhance detection models of PV defective modes [220]. Nonetheless, the precise extraction of series and shunt resistance values is challenging [218,219] and thus many researchers, e.g., [221–225], have developed approaches to optimise extraction techniques to estimate their range values. While accurate parameter extraction might be challenging, estimating their values' range is still vital for the healthy operation of PV modules.

Shunt resistance offers a pathway for photogenerated current, allowing it to bypass the PV equivalent circuit, whereas series resistance infers the solar cell component resistance altogether, such as the cell base and busbar resistance. Series resistance increases in the presence of PV failures or degradation. It has been claimed that degradation mechanisms influencing series resistance are the most prevalent degradation mechanisms after EVA discolouration [226]. Moreover, these have greater severity; Wohlgemuth and Kurtz [42] stated that increases in series resistance in PV modules may lead to disastrous consequences, resulting in fires. In contrast, a higher value of shunt resistance indicates a safe operation of the PV cell as it directs most of the generated photocurrents to flow through one healthy path [71,227]. However, when current is lost through alternative paths, R_{sh} reduces significantly, which ultimately leads to a severe drop in overall power production [71,227,228].

Kaplani and Kaplanis [229] investigated PV panels that were deployed for twenty years. They discovered that an 80% reduction in R_{sh} and a 50% increment in R_s were strongly linked to the PV panel's degradation, leading to 11% power loss. Furthermore, power degradation occurred as a result of several failures that directly impacted and reduced shunt resistance, including soldering defects, microcracks, shading, and hotspots [230,231]. Most of these failures were found to directly impact and increase series resistance, too [226,232,233]. It can be noted that the majority of PV defects summarised by Tsanakas et al. [56], particularly the electrical ones, have been found in the literature to decrease R_{sh} and increase R_S. Based on this, as well as on other findings, e.g., [88,220], shunt as well as series resistance appear as strong predictors of PV failures and deterioration. Optical failures such as EVA delamination were found to lower shunt resistance and increase series resistance. Gxasheka et al. [234] compared the parameters of five deployed PV modules. The one affected by delamination had approximately 50% lower shunt resistance accompanied by a 61% increment in series resistance.

The effect of encapsulant discolouration, the most prevalent EVA defect, was also determined by Rajput et al. [235] to decrease shunt resistance. However, a study by Sinha et al. [231] compared two module pairs that operated for 20 years in India; one in each pair had brown EVA discolouration. They assumed there was no evident link found between brown EVA discolouration and shunt resistance decrement. This is perhaps due to the

PV module receiving less illumination when EVA is discoloured [168] and, as stated by Ruschel et al. [236], shunt resistance increases when solar illumination decreases. However, this can be applied if EVA experiences the same discolouration level across the PV module. Otherwise, different levels of EVA discolouration might have the same effect as minor shading and will lead eventually to decreased shunt resistance.

On the other hand, electrical failures which are unlikely to be spotted by the naked eye [56], such as microcrack failures, were found by Zhang et al. [237] to decrease R_{sh} significantly. In their study, low shunt resistance was spotted in the short-circuit current slope in the *I*–*V* curve of a module with cracked cells, whereas the increment in series resistance was minor unless the range of irradiance was between 250 and 475 W m^{-2} [238]. Saavedra et al. [133] also experimentally investigated PV modules with cracked cells and reached the same conclusion as Zhang et al. [237], but noted a greater increment in R_S. Potential-induced degradation was also directly linked with shunt resistance reduction and series resistance increment [238–240]. Myer and Dyk [70] simulated a PV module that consisted of 36 cells with 30% of the cells under shading failure to analyse the effect of shading on electrical parameters. In their findings, both shading and hotspots, when present, significantly lowered shunt resistance.

Degradation and many PV failures were associated with low shunt resistance and increased series resistance, making it vital to explore their behaviours when the solar cell degrades. A MATLAB study conducted by Dhass et al. [241] showed that a reduction in shunt resistance caused a significant decrease in short-circuit current compared with open-circuit voltage. Another software program was employed by Dyk and Meyer [242] for shunt resistance reduction effects. They found that a decrement in shunt resistance reduced P_{MAX}, V_{OC}, and fill factor, with a slight increase in I_{SC}. Conversely, Sarkar [243] simulated the effect of a reduction in R_{sh} using SPICE and showed that a reduction in shunt resistance leads to a greater decrement in open-circuit voltage instead of short-circuit current. It can be noted that the outcome discrepancies were due to the studies [241–243] relying on simulation software programs.

Several practical experiments have also been conducted and published in the literature; back in 1969, Kennerud [244] investigated a cadmium sulphide (CdS) solar cell, applying the Newton–Raphson technique to solve the *I*–*V* equations. Then, he manipulated the electrical parameters, including R_{sh} and R_s, to examine their influence on *I*–*V* characteristics. The findings were experimentally verified and it was demonstrated that a decrease in shunt resistance was associated with a reduction in open-circuit voltage, while increasing series resistance was linked to a reduction in fill factor. Rummel et al. [245] fabricated a twelve-cell monocrystalline module to explore the effect of 24 scenarios of shunt resistance levels at different irradiance levels, falling from 1000 W m^{-2} down to 90 W m^{-2}. A significant drop in the module's efficiency was observed after reducing shunt resistance, particularly at the lowest shunt resistance level. With the assistance of electroluminescence (EL) imaging techniques, Roy and Gupta [228] investigated images of solar cells exhibiting low shunt resistance levels linked with faulty operations such as hotspots. Shunt resistance was reduced artificially to six levels from 0.3 kΩ to 0.001 kΩ. The results showed darker images for cells with reduced R_{sh}, with the level of darkness becoming more intense with the lowest levels of shunt resistance.

To sum up, it can be noticed from the literature that numerous studies have been conducted to explore the effects of shunt and series resistance as they are directly linked to most PV failures. Despite that, not as many studies employ them as indicators or predictors in the detection of PV failures or degradation, and the studies that do so are predominantly related to series resistance. Al Mahdi et al. [246,247] filled the gap in knowledge of shunt resistance in terms of PV degradation by developing a lab experiment that gradually and artificially decreased the shunt resistance of polycrystalline solar cells to propose a detection model. It was found that critical degradation of PV cells occurred when shunt resistance decreased to 100 Ω cm^2. Further experimental investigations for employing shunt and series resistance are needed to arrive at comprehensive and robust detection techniques for

PV failures. Table 5 lists the most recent review studies about some detection techniques of PV failure mechanisms.

Table 5. Most recent review studies of some detection techniques.

Detection Technique	Highlight	Ref.
Infrared Imaging (IR)	How PV benefits from IR and what can be done to expand IR application in PV with the assistance of machine learning models.	[191]
Electroluminescence (EL) and Deep Learning	A brief review of EL imaging in detecting microcrack failure modes with useful comparison to IR technique and the feasibility of using them in artificial intelligence models.	[248]
Machine Learning	Review of ML studies underlining their accuracy in detecting PV failure modes and highlighting common models, namely super vector (SVM) and neural network (ANN).	[249]
Deep Learning	Comparing deep learning models, their pros and cons, as well as proposing a future path for enhancement.	[250]
Electrical Characterisation	Reviewing and comparing detection techniques in grid-connected PV plants.	[251]

6. Conclusions

This review has captured a body of knowledge by highlighting the global growth in PV module deployment, stressing the need for understanding the reported PV failure behaviours and how they are initiated. When they occur, they lead to higher degradation rates, causing a significant reduction in power output and, in the worst-case scenario, may become catastrophic. Most literature reviews of PV failures are based on the severity and frequency of occurrence of failures. This review takes a different perspective and focuses on failure mechanisms based on PV module components, reviewing each component's susceptibility to failures.

Looking into the literature in depth allows for extracting the root cause of some failure and degradation mechanisms. For instance, UV, one of the environmental stress factors, is considered the root cause of the most common degradation, i.e., encapsulant EVA discolouration, which is responsible for the emergence of most optical failures, such as corrosion and delamination. Shading, glass breakage, and soldering defects, on the other hand, can cause hotspot failures. Most PV degradation mechanisms may lead to disastrous consequences, including human fatalities, when undetected or neglected.

In terms of failure detection techniques, it was pointed out that these should be simple, applicable to most PV systems, cost-effective, accurate, and able to detect failures at low solar irradiance levels. Typically, detection starts with visual inspection and then employs more instrumental methods such as infrared imaging. However, these devices are costly, require more labour, and are time-consuming and uncomprehensive, i.e., designed only to detect limited types of failures. In contrast, electrical characterisation, which includes monitoring the power or the *I*–*V* curve, infers most PV failures from shifts in the produced parameters. That would explain why it is the most common detection technique. Electrical characterisation detection techniques were detailed in several reviews, but there is a gap in engaging shunt and series resistance. This review details their effect, evaluating the possibilities for using them in electrical characterisation. This in turn paves the road for future studies to investigate *I*–*V* measurements under changes in shunt and series resistance, thereby enabling the development of models in a simple, applicable, comprehensive, and novel way to facilitate early intervention and avoid catastrophic deterioration.

Another future direction involves reviewing the available studies for preventive measures and recommended corrective actions for the failures listed in this review, evaluating their cost and feasibility of implementation in PV modules.

Funding: Hussain Al Mahdi would like to acknowledge PhD funding support from the Saudi Ministry of Education.

Conflicts of Interest: The authors declare no conflict of interest.

Abbreviations

AM1.5G	Standard solar spectrum
EVA	Ethylene vinyl acetate
FF	Fill factor of the solar cell
G	Solar irradiance
I_{01}	First saturation current of the solar cell
I_{02}	Second saturation current of the solar cell
I_m	Maximum current output at the solar cell's current–voltage curve
I_{SC}	Short-circuit current of the solar cell
IR	Infrared imaging
I–V	Current–voltage curve of the solar cell
J-box	Junction box, a component of photovoltaic modules
PDMS	Polydimethylsiloxane, a type of polymer used as an encapsulant in photovoltaic modules
PET	Polyethylene terephthalate, a plastic material used as the backsheet in photovoltaic modules
PID	Potential-induced degradation
P_{max}	Maximum power output, the maximal power produced by the solar cell
PV	Photovoltaic
RPN	Risk priority number used for rating guidelines
R_{sh}	Shunt or parallel resistance of the photovoltaic solar cell
R_s	Series resistance of the solar cell
SPICE	Simulation program with integrated circuit emphasis
STC	Standard test condition
TPU	Thermoplastic polyurethane
UV	Ultraviolet
V_{OC}	Open-circuit voltage of the solar cell
V_m	Maximum voltage output at the solar cell's current–voltage curve

References

1. Li, L.; Lin, J.; Wu, N.; Xie, S.; Meng, C.; Zheng, Y.; Wang, X.; Zhao, Y. Review and outlook on the international renewable energy development. *Energy Built Environ.* **2022**, *3*, 139–157. [CrossRef]
2. Green, M.A. How did solar cells get so cheap? *Joule* **2019**, *3*, 631–633. [CrossRef]
3. *PSE Projects, Photovoltaics Report*; Fraunhofer Institute for Solar Energy Systems ISE: Freiburg im Breisgau, Germany, 2022.
4. IEA. *Net Renewable Capacity Additions by Technology, 2020–2022*; IEA: Paris, France, 2021.
5. Goetzberger, A.; Hebling, C.; Schock, H.-W. Photovoltaic materials, history, status and outlook. *Mater. Sci. Eng. R Rep.* **2003**, *40*, 1–46. [CrossRef]
6. Green, M.A.; Dunlop, E.D.; Hohl-Ebinger, J.; Yoshita, M.; Kopidakis, N.; Ho-Baillie, A.W. Solar cell efficiency tables (version 55). *Prog. Photovolt. Res. Appl.* **2019**, *28*, 3–15. [CrossRef]
7. Peike, C.; Hädrich, I.; Weiß, K.-A.; Dürr, I. Overview of PV module encapsulation materials. *Photovolt. Int.* **2013**, *19*, 85–92.
8. Ma, S.; Yuan, G.; Zhang, Y.; Yang, N.; Li, Y.; Chen, Q. Development of encapsulation strategies towards the commercialization of perovskite solar cells. *Energy Environ. Sci.* **2022**, *15*, 13–55. [CrossRef]
9. Wang, H.; Cheng, X.; Yang, H.; He, W.; Chen, Z.; Xu, L.; Song, D. Potential-induced degradation: Recombination behavior, temperature coefficients and mismatch losses in crystalline silicon photovoltaic power plant. *Sol. Energy* **2019**, *188*, 258–264. [CrossRef]
10. Vázquez, M.; Rey-Stolle, I. Photovoltaic module reliability model based on field degradation studies. *Prog. Photovolt. Res. Appl.* **2008**, *16*, 419–433. [CrossRef]

11. Daher, D.H.; Gaillard, L.; Ménézo, C. Experimental assessment of long-term performance degradation for a PV power plant operating in a desert maritime climate. *Renew. Energy* **2022**, *187*, 44–55. [CrossRef]
12. Wohlgemuth, J. *IEC 61215: What It Is and Isn't (Presentation)*; National Renewable Energy Lab (NREL): Golden, CO, USA, 2012.
13. Barretta, C.; Macher, A.E.; Ascencio-Vásquez, J.; Köntges, M.; Topič, M.; Oreski, G. Degradation of Crystalline Silicon Photovoltaic Modules Installed in Different Climates. In Proceedings of the IEEE 49th Photovoltaics Specialists Conference (PVSC) 2022, Philadelphia, PA, USA, 5–10 June 2022; pp. 680–682.
14. Dhimish, M.; Tyrrell, A.M. Power loss and hotspot analysis for photovoltaic modules affected by potential induced degradation. *NPJ Mater. Degrad.* **2022**, *6*, 11. [CrossRef]
15. Köntges, M.; Kurtz, S.; Packard, C.; Jahn, U.; Berger, K.A.; Kato, K.; Friesen, T.; Liu, H.; Van Iseghem, M. Review of Failures of Photovoltaic Modules IEA PVPS Task 13 External Final Report March 2014. IEA-PVPS T13-01. 2014. Available online: https://iea-pvps.org/wp-content/uploads/2020/01/IEA-PVPS_T13-01_2014_Review_of_Failures_of_Photovoltaic_Modules_Final.pdf (accessed on 3 August 2023).
16. Jordan, D.C.; Silverman, T.J.; Wohlgemuth, J.H.; Kurtz, S.R.; VanSant, K.T. Photovoltaic failure and degradation modes. *Prog. Photovolt. Res. Appl.* **2017**, *25*, 318–326. [CrossRef]
17. Madeti, S.R.; Singh, S. A comprehensive study on different types of faults and detection techniques for solar photovoltaic system. *Sol. Energy* **2017**, *158*, 161–185. [CrossRef]
18. Pillai, D.S.; Rajasekar, N. A comprehensive review on protection challenges and fault diagnosis in PV systems. *Renew. Sustain. Energy Rev.* **2018**, *91*, 18–40. [CrossRef]
19. Osmani, K.; Haddad, A.; Lemenand, T.; Castanier, B.; Alkhedher, M.; Ramadan, M. A critical review of PV systems' faults with the relevant detection methods. *Energy Nexus* **2023**, *12*, 100257. [CrossRef]
20. Jordan, D.C.; Sekulic, B.; Marion, B.; Kurtz, S.R. Performance and aging of a 20-year-old silicon PV system. *IEEE J. Photovolt.* **2015**, *5*, 744–751. [CrossRef]
21. Han, H.; Dong, X.; Li, B.; Yan, H.; Verlinden, P.J.; Liu, J.; Huang, J.; Liang, Z.; Shen, H. Degradation analysis of crystalline silicon photovoltaic modules exposed over 30 years in hot-humid climate in China. *Sol. Energy* **2018**, *170*, 510–519. [CrossRef]
22. Ndiaye, A.; Charki, A.; Kobi, A.; Kébé, C.M.F.; Ndiaye, P.A.; Sambou, V. Degradations of silicon photovoltaic modules: A literature review. *Sol. Energy* **2013**, *96*, 140–151. [CrossRef]
23. Triki-Lahiani, A.; Abdelghani, A.B.-B.; Slama-Belkhodja, I. Fault detection and monitoring systems for photovoltaic installations: A review. *Renew. Sustain. Energy Rev.* **2018**, *82*, 2680–2692. [CrossRef]
24. Bai, A.; Popp, J.; Balogh, P.; Gabnai, Z.; Pályi, B.; Farkas, I.; Pintér, G.; Zsiborács, H. Technical and economic effects of cooling of monocrystalline photovoltaic modules under Hungarian conditions. *Renew. Sustain. Energy Rev.* **2016**, *60*, 1086–1099. [CrossRef]
25. Aboagye, B.; Gyamfi, S.; Ofosu, E.A.; Djordjevic, S. Investigation into the impacts of design, installation, operation and maintenance issues on performance and degradation of installed solar photovoltaic (PV) systems. *Energy Sustain. Dev.* **2022**, *66*, 165–176. [CrossRef]
26. Jordan, D.C.; Kurtz, S.R.; VanSant, K.; Newmiller, J. Compendium of photovoltaic degradation rates. *Prog. Photovolt. Res. Appl.* **2016**, *24*, 978–989. [CrossRef]
27. Colvin, D.J.; Iqbal, N.; Yerger, J.H.; Li, F.; Sinha, A.; Vicnansky, G.; Brummer, G.; Zheng, N.; Schneller, E.J.; Barkaszi, J. Degradation of monocrystalline silicon photovoltaic modules from a 10-year-old rooftop system in Florida. *IEEE J. Photovolt.* **2023**, *13*, 275–282. [CrossRef]
28. Golive, Y.R.; Zachariah, S.; Dubey, R.; Chattopadhyay, S.; Bhaduri, S.; Singh, H.K.; Bora, B.; Kumar, S.; Tripathi, A.K.; Kottantharayil, A. Analysis of field degradation rates observed in all-India survey of photovoltaic module reliability 2018. *IEEE J. Photovolt.* **2019**, *10*, 560–567. [CrossRef]
29. Quansah, D.A.; Adaramola, M.S. Ageing and degradation in solar photovoltaic modules installed in northern Ghana. *Sol. Energy* **2018**, *173*, 834–847. [CrossRef]
30. Bansal, N.; Jaiswal, S.P.; Singh, G. Long term operational performance and experimental on-field degradation measurement of 10 MW PV plant in remote location in India. *Energy Sustain. Dev.* **2022**, *67*, 135–150. [CrossRef]
31. Bansal, N.; Jaiswal, S.P.; Singh, G. Prolonged degradation and reliability assessment of installed modules operational for 10 years in 5 MW PV plant in hot semi-arid climate. *Energy Sustain. Dev.* **2022**, *68*, 373–389. [CrossRef]
32. Aboagye, B.; Gyamfi, S.; Ofosu, E.A.; Djordjevic, S. Characterisation of visual defects on installed solar photovoltaic (pv) modules in different climatic zones in Ghana. *Sci. Afr.* **2023**, *20*, e01682. [CrossRef]
33. Chekal Affari, B.; Kahoul, N.; Haouam, A.; Cheghib, H.; Necaibia, A.; Younes, M.; Kherici, Z. Power losses in PV arrays of field-aged modules. *Microelectron. Reliab.* **2023**, *147*, 115052. [CrossRef]
34. Belhaouas, N.; Mehareb, F.; Kouadri-Boudjelthia, E.; Assem, H.; Bensalem, S.; Hadjrioua, F.; Aissaoui, A.; Hafdaoui, H.; Chahtou, A.; Bakria, K. The performance of solar PV modules with two glass types after 11 years of outdoor exposure under the mediterranean climatic conditions. *Sustain. Energy Technol. Assess.* **2022**, *49*, 101771. [CrossRef]
35. Faye, I.; Ndiaye, A.; Camara, M.; Geke, R.; Blieske, U.; Thiame, M.; Kobor, D. Investigation of Crystalline Silicon Photovoltaic Modules Degradation after 14 years Outdoor Exposure in Cologne Climate (Germany) by Electroluminescence (EL) and Infrared (IR). In Proceedings of the 52nd American Solar Energy Society National Solar Conference 2023, Cham, Germany, 8–11 August 2023; pp. 105–113.

36. Segbefia, O.K.; Akhtar, N.; Sætre, T.O. Defects and fault modes of field-aged photovoltaic modules in the Nordics. *Energy Rep.* **2023**, *9*, 3104–3119. [CrossRef]
37. Segbefia, O.K.; Akhtar, N.; Sætre, T.O. Moisture induced degradation in field-aged multicrystalline silicon photovoltaic modules. *Sol. Energy Mater. Sol. Cells* **2023**, *258*, 112407. [CrossRef]
38. Olivencia Polo, F.A.; Ferrero Bermejo, J.; Gómez Fernández, J.F.; Crespo Márquez, A. Failure mode prediction and energy forecasting of PV plants to assist dynamic maintenance tasks by ANN based models. *Renew. Energy* **2015**, *81*, 227–238. [CrossRef]
39. Sepanski, A.; Reil, F.; Vaaßen, W.; Janknecht, E.; Hupach, U.; Bogdanski, N.; van Heeckeren, B. Assessing Fire Risks in Photovoltaic Systems and Developing Safety Concepts for Risk Minimization. 2018. Available online: https://www.energy.gov/eere/solar/articles/assessing-fire-risks-photovoltaic-systems-and-developing-safety-concepts-risk (accessed on 3 August 2023).
40. Cancelliere, P. PV electrical plants fire risk assessment and mitigation according to the Italian national fire services guidelines. *Fire Mater.* **2016**, *40*, 355–367. [CrossRef]
41. Mohd Nizam Ong, N.A.F.; Mohd Tohir, M.Z.; Mutlak, M.M.; Sadiq, M.A.; Omar, R.; Md Said, M.S. BowTie analysis of rooftop grid-connected photovoltaic systems. *Process Saf. Prog.* **2022**, *41*, S106–S117. [CrossRef]
42. Wohlgemuth, J.H.; Kurtz, S.R. How can we make PV modules safer? In Proceedings of the 2012 38th IEEE Photovoltaic Specialists Conference, Austin, TX, USA, 3–8 June 2012; pp. 3162–3165.
43. Aram, M.; Zhang, X.; Qi, D.; Ko, Y. A State-of-the-Art Review of Fire Safety of Photovoltaic Systems in Buildings. *J. Clean. Prod.* **2021**, *308*, 127239. [CrossRef]
44. Blazey, S. *Fire and Solar PV Systems–Investigations and Evidence*; Report Number: P100874-1004; July; 2017; Available online: https://helios-om.com/wp-content/uploads/2020/07/Fires_and_solar_PV_systems-Investigations_Evidence_Issue_2.9.pdf (accessed on 5 August 2023).
45. Wu, Z.; Hu, Y.; Wen, J.X.; Zhou, F.; Ye, X. A review for solar panel fire accident prevention in large-scale PV applications. *IEEE Access* **2020**, *8*, 132466–132480. [CrossRef]
46. Schulze, K.; Groh, M.; Nieß, M.; Vodermayer, C.; Wotruba, G.; Becker, G. Untersuchung von Alterungseffekten bei monokristallinen PV-Modulen mit mehr als 15 Betriebsjahren durch Elektrolumineszenz-und Leistungsmessung. In Proceedings of the 28th Symposium Photovoltaische Solarenergie, Frankfurt, Germany, 24–28 September 2012.
47. Jordan, D.C.; Kurtz, S.R. Photovoltaic degradation rates—An analytical review. *Prog. Photovolt. Res. Appl.* **2013**, *21*, 12–29. [CrossRef]
48. Durand, S.; Bowling, D. *Field Experience with Photovoltaic Systems: Ten-Year Assessment*; Final Report; Electric Power Research Inst.: Palo Alto, CA, USA; Southwest: Dallas, TX, USA, 1993.
49. *IEC 60050-191*; International Electrotechnical Vocabulary: Chapter 191: Dependability and Quality of Service. International Electrotechnical Commission: Geneva, Switzerland, 1990.
50. Jordan, D.; Haegel, N.; Barnes, T. Photovoltaics module reliability for the terawatt age. *Prog. Energy* **2022**, *4*, 022002. [CrossRef]
51. Romero-Fiances, I.; Livera, A.; Theristis, M.; Makrides, G.; Stein, J.S.; Nofuentes, G.; de la Casa, J.; Georghiou, G.E. Impact of duration and missing data on the long-term photovoltaic degradation rate estimation. *Renew. Energy* **2022**, *181*, 738–748. [CrossRef]
52. Heywang, W.; Zaininger, K.H. Silicon: The semiconductor material. In *Silicon*; Springer: Berlin/Heidelberg, Germany, 2004; pp. 25–42.
53. Kılıç, A.; Öztürk, A. *Güneş Enerjisi*; Kipaş Dağıtımcılık: Istanbul, Turkey, 1983.
54. Gürtürk, M.; Benli, H.; Ertürk, N.K. Determination of the effects of temperature changes on solar glass used in photovoltaic modules. *Renew. Energy* **2020**, *145*, 711–724. [CrossRef]
55. Afridi, M.; Kumar, A.; ibne Mahmood, F.; Tamizhmani, G. Hotspot testing of glass/backsheet and glass/glass PV modules pre-stressed in extended thermal cycling. *Sol. Energy* **2023**, *249*, 467–475. [CrossRef]
56. Tsanakas, J.A.; Ha, L.; Buerhop, C. Faults and infrared thermographic diagnosis in operating c-Si photovoltaic modules: A review of research and future challenges. *Renew. Sustain. Energy Rev.* **2016**, *62*, 695–709. [CrossRef]
57. Enaganti, P.K.; Bhattacharjee, A.; Ghosh, A.; Chanchangi, Y.N.; Chakraborty, C.; Mallick, T.K.; Goel, S. Experimental investigations for dust build-up on low-iron glass exterior and its effects on the performance of solar PV systems. *Energy* **2022**, *239*, 122213. [CrossRef]
58. Tagawa, K.; Kutani, A.; Qinglin, P. Effect of sand erosion of glass surface on performances of photovoltaic module. In Proceedings of the Sustainable Research and Innovation Conference, Nairobi, Kenya, 5–7 October 2022; pp. 75–77.
59. King, D.; Quintana, M.; Kratochvil, J.; Ellibee, D.; Hansen, B. Photovoltaic module performance and durability following long-term field exposure. *Prog. Photovolt. Res. Appl.* **2000**, *8*, 241–256. [CrossRef]
60. King, D.; Pern, F.; Pitts, J.; Bingham, C.; Czanderna, A. Optical changes in cerium-containing glass as a result of accelerated exposure testing [of PV modules]. In Proceedings of the Conference Record of the Twenty Sixth IEEE Photovoltaic Specialists Conference-1997, Anaheim, CA, USA, 29 September–3 October 1997; pp. 1117–1120.
61. Kempe, M.D.; Moricone, T.; Kilkenny, M. Effects of cerium removal from glass on photovoltaic module performance and stability. In Proceedings of the Reliability of Photovoltaic Cells, Modules, Components, and Systems II; SPIE: Bellingham, DC, USA, 2009; p. 74120Q.

62. Quansah, D.A.; Adaramola, M.S. Comparative study of performance degradation in poly- and mono-crystalline-Si solar PV modules deployed in different applications. *Int. J. Hydrogen Energy* **2018**, *43*, 3092–3109. [CrossRef]
63. Dietrich, S.; Pander, M.; Ebert, M.; Bagdahn, J. Mechanical assessment of large photovoltaic modules by test and finite element analysis. In Proceedings of the 23rd European Photovoltaic Solar Energy Conference, Valencia, Spain, 1–5 September 2008.
64. Cavieres, R.; Barraza, R.; Estay, D.; Bilbao, J.; Valdivia-Lefort, P. Automatic soiling and partial shading assessment on PV modules through RGB images analysis. *Appl. Energy* **2022**, *306*, 117964. [CrossRef]
65. Bora, B.; Sastry, O.S.; Kumar, R.; Dubey, R.; Chattopadhyay, S.; Vasi, J.; Mondal, S.; Prasad, B. Failure mode analysis of PV modules in different climatic conditions. *IEEE J. Photovolt.* **2020**, *11*, 453–460. [CrossRef]
66. Chandel, S.S.; Nagaraju Naik, M.; Sharma, V.; Chandel, R. Degradation analysis of 28 year field exposed mono-c-Si photovoltaic modules of a direct coupled solar water pumping system in western Himalayan region of India. *Renew. Energy* **2015**, *78*, 193–202. [CrossRef]
67. Titu-Marius, B. Some reliability aspects of photovoltaic modules. In *Reliability and Ecological Aspects of Photovoltaic Modules*; IntechOpen: Rijeka, Croatia, 2020.
68. Castaner, L.; Silvestre, S. *Modelling Photovoltaic Systems Using PSpice*; John Wiley and Sons: Hoboken, NJ, USA, 2002.
69. Deng, S.; Zhang, Z.; Ju, C.; Dong, J.; Xia, Z.; Yan, X.; Xu, T.; Xing, G. Research on hot spot risk for high-efficiency solar module. *Energy Procedia* **2017**, *130*, 77–86. [CrossRef]
70. Meyer, E.L.; Van Dyk, E.E. The effect of reduced shunt resistance and shading on photovoltaic module performance. In Proceedings of the Conference Record of the Thirty-First IEEE Photovoltaic Specialists Conference, Lake Buena Vista, FL, USA, 3–7 January 2005; pp. 1331–1334.
71. Vankadara, S.K.; Chatterjee, S.; Balachandran, P.K. An accurate analytical modeling of solar photovoltaic system considering Rs and Rsh under partial shaded condition. *Int. J. Syst. Assur. Eng. Manag.* **2022**, *13*, 2472–2481. [CrossRef]
72. Ghanbari, T. Permanent partial shading detection for protection of photovoltaic panels against hot spotting. *IET Renew. Power Gener.* **2016**, *11*, 123–131. [CrossRef]
73. Jadin, M.S.B.; Safian, S.F.A.; Ghazali, K.H.; Ven, T.L.; Shah, A.S.M. Hotspot Detection in Photovoltaic Array Using Thermal Imaging Method. In Proceedings of the 6th International Conference on Electrical, Control and Computer Engineering, Kuantan, Malaysia, 23 August 2022; pp. 101–107.
74. Hossion, M.A. Visual and electrical degradation data of five years aged rooftop photovoltaic modules. *Data Brief* **2020**, *31*, 105762. [CrossRef] [PubMed]
75. Hasan, O.; Arif, A. Performance and life prediction model for photovoltaic modules: Effect of encapsulant constitutive behavior. *Sol. Energy Mater. Sol. Cells* **2014**, *122*, 75–87. [CrossRef]
76. Miller, D.C.; Bokria, J.G.; Burns, D.M.; Fowler, S.; Gu, X.; Hacke, P.L.; Honeker, C.C.; Kempe, M.D.; Köhl, M.; Phillips, N.H. Degradation in photovoltaic encapsulant transmittance: Results of the first PVQAT TG5 artificial weathering study. *Prog. Photovolt. Res. Appl.* **2019**, *27*, 391–409. [CrossRef]
77. López-Escalante, M.; Caballero, L.J.; Martín, F.; Gabás, M.; Cuevas, A.; Ramos-Barrado, J. Polyolefin as PID-resistant encapsulant material in PV modules. *Sol. Energy Mater. Sol. Cells* **2016**, *144*, 691–699. [CrossRef]
78. Kempe, M. Overview of scientific issues involved in selection of polymers for PV applications. In Proceedings of the 2011 37th IEEE Photovoltaic Specialists Conference, Seattle, WA, USA, 19–24 June 2011; pp. 000085–000090.
79. Habersberger, B.M.; Hacke, P.; Madenjian, L.S. Evaluation of the PID-s susceptibility of modules encapsulated in materials of varying resistivity. In Proceedings of the 2018 IEEE 7th World Conference on Photovoltaic Energy Conversion (WCPEC) (A Joint Conference of 45th IEEE PVSC, 28th PVSEC & 34th EU PVSEC), Amsterdam, The Netherlands, 10–15 June 2018; pp. 3807–3809.
80. Kapur, J.; Stika, K.M.; Westphal, C.S.; Norwood, J.L.; Hamzavytehrany, B. Prevention of potential-induced degradation with thin ionomer film. *IEEE J. Photovolt.* **2014**, *5*, 219–223. [CrossRef]
81. Azam, M.F.; Shahzad, N.; Rafique, A.; Ayub, M.; Khalid, H.A.; Waqas, A. Accelerated UV stress testing and characterization of PV-modules: Reliability analysis using different encapsulants and glass sheets. *Sustain. Energy Technol. Assess.* **2023**, *56*, 103119. [CrossRef]
82. Peike, C.; Purschke, L.; Weiss, K.-A.; Köhl, M.; Kempe, M. Towards the origin of photochemical EVA discoloration. In Proceedings of the 2013 IEEE 39th Photovoltaic Specialists Conference (PVSC), Tampa, FL, USA, 16–21 June 2013; pp. 1579–1584.
83. Kyranaki, N.; Smith, A.; Yendall, K.; Hutt, D.A.; Whalley, D.C.; Gottschalg, R.; Betts, T.R. Damp-heat induced degradation in photovoltaic modules manufactured with passivated emitter and rear contact solar cells. *Prog. Photovolt. Res. Appl.* **2022**, *30*, 1061–1071. [CrossRef]
84. Badiee, A.; Ashcroft, I.; Wildman, R.D. The thermo-mechanical degradation of ethylene vinyl acetate used as a solar panel adhesive and encapsulant. *Int. J. Adhes. Adhes.* **2016**, *68*, 212–218. [CrossRef]
85. Desai, U.; Sharma, B.K.; Singh, A.; Singh, A. A comparison of evolution of adhesion mechanisms and strength post damp-heat aging for a range of VA content in EVA encapsulant with photovoltaic backsheet. *Sol. Energy* **2022**, *231*, 908–920. [CrossRef]
86. Lathrop, J.W.; Hartman, R.A.; Saylor, C.R. Investigation of Reliability Attributes and Accelerated Stress Factors on Terrestrial Solar Cells. 1981. Available online: https://ntrs.nasa.gov/citations/19810011041 (accessed on 3 August 2023).

87. Bansal, N.; Jaiswal, S.P.; Singh, G. Comparative investigation of performance evaluation, degradation causes, impact and corrective measures for ground mount and rooftop solar PV plants—A review. *Sustain. Energy Technol. Assess.* **2021**, *47*, 101526. [CrossRef]
88. Manganiello, P.; Balato, M.; Vitelli, M. A survey on mismatching and aging of PV modules: The closed loop. *IEEE Trans. Ind. Electron.* **2015**, *62*, 7276–7286. [CrossRef]
89. Stark, W.; Jaunich, M. Investigation of Ethylene/Vinyl Acetate Copolymer (EVA) by thermal analysis DSC and DMA. *Polym. Test.* **2011**, *30*, 236–242. [CrossRef]
90. Gok, A.; Gordon, D.A.; Wang, M.; French, R.H.; Bruckman, L.S. Degradation Science and Pathways in PV Systems. In *Durability and Reliability of Polymers and Other Materials in Photovoltaic Modules*; Elsevier: Amsterdam, The Netherlands, 2019; pp. 47–93.
91. Perret-Aebi, L.E.; Li, H.Y.; Théron, R.; Roeder, G.; Luo, Y.; Turlings, T.; Lange, R.F.M.; Ballif, C. Insights on EVA lamination process: Where do the Bubbles Come from. In Proceedings of the 25th European Photovoltaic Solar Energy Conference and Exhibition, Valencia, Spain, 6–10 September 2010.
92. Karthikeyan, S.; Ajay, G.B.; Ahamed, N.R.; Sharun, A. Edge AI–Based Aerial Monitoring. In *Applied Edge AI: Concepts, Platforms, and Industry Use Cases*; Auerbach Publications: Boca Raton, FL, USA; CRC Press: Boca Raton, FL, USA, 2022.
93. Shrestha, S.M.; Mallineni, J.K.; Yedidi, K.R.; Knisely, B.; Tatapudi, S.; Kuitche, J.; TamizhMani, G. Determination of dominant failure modes using FMECA on the field deployed c-Si modules under hot-dry desert climate. *IEEE J. Photovolt.* **2014**, *5*, 174–182. [CrossRef]
94. Rajput, P.; Tiwari, G.N.; Sastry, O.S.; Bora, B.; Sharma, V. Degradation of mono-crystalline photovoltaic modules after 22 years of outdoor exposure in the composite climate of India. *Sol. Energy* **2016**, *135*, 786–795. [CrossRef]
95. de Oliveira, M.C.C.; Cardoso, A.S.A.D.; Viana, M.M.; Lins, V.d.F.C. The causes and effects of degradation of encapsulant ethylene vinyl acetate copolymer (EVA) in crystalline silicon photovoltaic modules: A review. *Renew. Sustain. Energy Rev.* **2018**, *81*, 2299–2317. [CrossRef]
96. Frederick, J.; Snell, H.; Haywood, E. Solar ultraviolet radiation at the earth's surface. *Photochem. Photobiol.* **1989**, *50*, 443–450. [CrossRef]
97. Klampaftis, E.; Congiu, M.; Robertson, N.; Richards, B.S. Luminescent ethylene vinyl acetate encapsulation layers for enhancing the short wavelength spectral response and efficiency of silicon photovoltaic modules. *IEEE J. Photovolt.* **2011**, *1*, 29–36. [CrossRef]
98. Kamel, M.S.A.; Oelgemöller, M.; Jacob, M.V. Sustainable plasma polymer encapsulation materials for organic solar cells. *J. Mater. Chem. A* **2022**, *10*, 4683–4694. [CrossRef]
99. Segbefia, O.K. Temperature profiles of field-aged photovoltaic modules affected by optical degradation. *Heliyon* **2023**, *9*, e19566. [CrossRef] [PubMed]
100. Holley, W.H.; Agro, S.C.; Galica, J.P.; Thoma, L.A.; Yorgensen, R.S.; Ezrin, M.; Klemchuk, P.; Lavigne, G. Investigation into the causes of browning in EVA encapsulated flat plate PV modules. In Proceedings of the 1994 IEEE 1st World Conference on Photovoltaic Energy Conversion-WCPEC (A Joint Conference of PVSC, PVSEC and PSEC), Waikoloa, HI, USA, 5–9 December 1994; pp. 893–896.
101. Jiang, S.; Wang, K.; Zhang, H.; Ding, Y.; Yu, Q. Encapsulation of PV modules using ethylene vinyl acetate copolymer as the encapsulant. *Macromol. React. Eng.* **2015**, *9*, 522–529. [CrossRef]
102. Noman, M.; Tu, S.; Ahmad, S.; Zafar, F.U.; Khan, H.A.; Rehman, S.U.; Waqas, M.; Khan, A.D.; Rehman, O.U. Assessing the reliability and degradation of 10–35 years field-aged PV modules. *PLoS ONE* **2022**, *17*, e0261066. [CrossRef] [PubMed]
103. Arularasu, P. *Combined UV-Temperature-Humidity Accelerated Testing of PV Modules: Reliability of UV-Cut and UV-Pass EVA Encapsulants*; Arizona State University: Tempe, AZ, USA, 2019.
104. *ISO 17223*; Plastics—Determination of Yellowness Index and Change in Yellowness Index. ISO: Geneva, Switzerland, 2014.
105. de Oliveira, M.C.C.; Cassini, D.A.; Diniz, A.S.A.C.; Soares, L.G.; Viana, M.M.; Kazmerski, L.L.; Lins, V.d.F.C. Comparison and analysis of performance and degradation differences of crystalline-Si photovoltaic modules after 15-years of field operation. *Sol. Energy* **2019**, *191*, 235–250. [CrossRef]
106. Yong, H.; Minemoto, T.; Takahashi, T. Dependence of Photovoltage on Incident Photon Energies Investigated by Photo-assisted Kelvin Probe Force Microscopy on Cu (In, Ga) Se 2 Solar Cells. In Proceedings of the 2018 IEEE 7th World Conference on Photovoltaic Energy Conversion (WCPEC) (A Joint Conference of 45th IEEE PVSC, 28th PVSEC & 34th EU PVSEC), Hilto Waikoloa Village, United States, 10–15 June 2018; pp. 1966–1969.
107. Adothu, B.; Chattopadhyay, S.; Bhatt, P.; Hui, P.; Costa, F.R.; Mallick, S. Early-stage identification of encapsulants photobleaching and discoloration in crystalline silicon photovoltaic module laminates. *Prog. Photovolt. Res. Appl.* **2020**, *28*, 767–778. [CrossRef]
108. Kaplani, E. Detection of degradation effects in field-aged c-Si solar cells through IR thermography and digital image processing. *Int. J. Photoenergy* **2012**, *2012*, 396792. [CrossRef]
109. Kurtz, S. *Photovoltaic Module Reliability Workshop*; National Renewable Energy Lab (NREL): Golden, CO, USA, 2014. [CrossRef]
110. Ferrara, C.; Philipp, D. Why Do PV Modules Fail? *Energy Procedia* **2012**, *15*, 379–387. [CrossRef]
111. Rosillo, F.; Alonso-Garcia, M. Evaluation of color changes in PV modules using reflectance measurements. *Sol. Energy* **2019**, *177*, 531–537. [CrossRef]

112. Pern, F.; Czanderna, A.; Emery, K.; Dhere, R. Weathering degradation of EVA encapsulant and the effect of its yellowing on solar cell efficiency. In Proceedings of the the Conference Record of the Twenty-Second IEEE Photovoltaic Specialists Conference-1991, Las Vegas, NV, USA, 7–11 October 1991; pp. 557–561.
113. Dechthummarong, C.; Wiengmoon, B.; Chenvidhya, D.; Jivacate, C.; Kirtikara, K. Physical deterioration of encapsulation and electrical insulation properties of PV modules after long-term operation in Thailand. *Sol. Energy Mater. Sol. Cells* **2010**, *94*, 1437–1440. [CrossRef]
114. Photovoltaic, C.S.T. Modules—Design Qualification and Type Approval. *IEC* **2005**, *1215*, 2005.
115. Diniz, A.S.A.; Cassini, D.A.; de Oliveira, M.C.; de Lins, V.F.; Viana, M.M.; Braga, D.S.; Kazmerski, L.L. Evaluation of Performance Losses and Degradation of Aged Crystalline Si Photovoltaic Modules Installed in Minas Gerais (Brazil). In *Renewable Energy and Sustainable Buildings*; Springer: Berlin/Heidelberg, Germany, 2020; pp. 29–46.
116. Dhimish, M. Micro cracks distribution and power degradation of polycrystalline solar cells wafer: Observations constructed from the analysis of 4000 samples. *Renew. Energy* **2020**, *145*, 466–477. [CrossRef]
117. Eslami Majd, A.; Ekere, N.N. Crack initiation and growth in PV module interconnection. *Sol. Energy* **2020**, *206*, 499–507. [CrossRef]
118. Grunow, P.; Clemens, P.; Hoffmann, V.; Litzenburger, B.; Podlowski, L. Influence of micro cracks in multi-crystalline silicon solar cells on the reliability of PV modules. In Proceedings of the 20th EUPVSEC, Barcelona, Spain, 6–10 June 2005; pp. 2042–2047.
119. BrightSpot Automation, L.L.C.; Westford, M.A. Solar panel design factors to reduce the impact of cracked cells and the tendency for crack propagation. In Proceedings of the NREL PV Module Reliability Workshop, Denver, CO, USA, 4 February 2015.
120. Sander, M.; Dietrich, S.; Pander, M.; Schweizer, S.; Ebert, M.; Bagdahn, J. Investigations on crack development and crack growth in embedded solar cells. *Reliab. Photovolt. Cells Modul. Compon. Syst. IV* **2011**, *8112*, 811209.
121. Buerhop, C.; Schlegel, D.; Vodermayer, C.; Nieß, M. Quality control of PV-modules in the field using infrared-thermography. In Proceedings of the 26th European Photovoltaic Solar Energy Conference, Hamburg, Germany, 5–9 September 2011; pp. 3894–3897.
122. Siruvuri, S.V.; Budarapu, P.R.; Paggi, M. Influence of cracks on fracture strength and electric power losses in Silicon solar cells at high temperatures: Deep machine learning and molecular dynamics approach. *Appl. Phys. A* **2023**, *129*, 408. [CrossRef]
123. Dhimish, M.; Holmes, V.; Mehrdadi, B.; Dales, M. The impact of cracks on photovoltaic power performance. *J. Sci. Adv. Mater. Devices* **2017**, *2*, 199–209. [CrossRef]
124. Sohail, A.; Ul Islam, N.; Ul Haq, A.; Ul Islam, S.; Shafi, I.; Park, J. Fault detection and computation of power in PV cells under faulty conditions using deep-learning. *Energy Rep.* **2023**, *9*, 4325–4336. [CrossRef]
125. Dolara, A.; Leva, S.; Manzolini, G.; Ogliari, E. Investigation on performance decay on photovoltaic modules: Snail trails and cell microcracks. *IEEE J. Photovolt.* **2014**, *4*, 1204–1211. [CrossRef]
126. Sinaga, R. Turnitin: A Preliminary Study of Common Defects of Photovoltaic Modules in West Timor, Indonesia. In Proceedings of the IOP Conference Series: Earth and Environmental Science 2020, Bogor, Indonesia, 1 July 2020; Volume 542, p. 012041.
127. Duerr, I.; Bierbaum, J.; Metzger, J.; Richter, J.; Philipp, D. Silver Grid Finger Corrosion on Snail Track affected PV Modules—Investigation on Degradation Products and Mechanisms. *Energy Procedia* **2016**, *98*, 74–85. [CrossRef]
128. Swanson, R.; Cudzinovic, M.; DeCeuster, D.; Desai, V.; Jürgens, J.; Kaminar, N.; Mulligan, W.; Rodrigues-Barbarosa, L.; Rose, D.; Smith, D. The surface polarization effect in high-efficiency silicon solar cells. In Proceedings of the 15th PVSEC, Shanghai, China, 10–15 October 2005.
129. Yamaguchi, S.; Masuda, A.; Marumoto, K.; Ohdaira, K. Mechanistic Understanding of Polarization-Type Potential-Induced Degradation in Crystalline-Silicon Photovoltaic Cell Modules. *Adv. Energy Sustain. Res.* **2023**, *4*, 2200167. [CrossRef]
130. Köntges, M.; Oreski, G.; Jahn, U.; Herz, M.; Hacke, P.; Weiß, K.-A. *Assessment of Photovoltaic Module Failures in the Field: International Energy Agency Photovoltaic Power Systems Programme: IEA PVPS Task 13, Subtask 3: Report IEA-PVPS T13-09: 2017*; International Energy Agency: Paris, France, 2017.
131. Pingel, S.; Janke, S.; Frank, O. Recovery methods for modules affected by potential induced degradation (PID). In Proceedings of the 27th European Photovoltaic Solar Energy Conference and Exhibition (Frankfurt), Frankfurt, Germany, 24–28 September 2012; pp. 3379–3383.
132. Molto, C.; Oh, J.; Mahmood, F.I.; Li, M.; Hacke, P.; Li, F.; Smith, R.; Colvin, D.; Matam, M.; DiRubio, C. Review of Potential-Induced Degradation in Bifacial Photovoltaic Modules. *Energy Technol.* **2023**, *11*, 2200943. [CrossRef]
133. Gallardo-Saavedra, S.; Hernández-Callejo, L.; del Carmen Alonso-García, M.; Santos, J.D.; Morales-Aragonés, J.I.; Alonso-Gómez, V.; Moretón-Fernández, Á.; González-Rebollo, M.Á.; Martínez-Sacristán, O. Nondestructive characterization of solar PV cells defects by means of electroluminescence, infrared thermography, I–V curves and visual tests: Experimental study and comparison. *Energy* **2020**, *205*, 117930. [CrossRef]
134. Köntges, M.; Kajari-Schröder, S.; Kunze, I. Cell cracks measured by UV fluorescence in the field. In Proceedings of the 27th EU PVSEC, Frankfurt, Germany, 24–28 September 2012; pp. 3033–3040.
135. Colvin, D.J.; Schneller, E.J.; Davis, K.O. Impact of interconnection failure on photovoltaic module performance. *Prog. Photovolt. Res. Appl.* **2021**, *29*, 524–532. [CrossRef]
136. Majd, A.E.; Ekere, N.N.; Darvazi, A.R.; Sedehi, A.A. Creep-fatigue lifetime estimation of efficient photovoltaic module ribbon interconnections. *Microelectron. Reliab.* **2022**, *139*, 114831. [CrossRef]

137. Köntges, M.; Altmann, S.; Heimberg, T.; Jahn, U.; Berger, K.A. Mean degradation rates in PV systems for various kinds of PV module failures. In Proceedings of the 32nd European Photovoltaic Solar Energy Conference and Exhibition, Munich, Germany, 20–24 June 2016; pp. 21–24.
138. Kurtz, S. *2017 NREL Photovoltaic Reliability Workshop*; National Renewable Energy Laboratory (NREL): Golden, CO, USA, 2017.
139. Illya, G.; Handara, V.; Siahandan, M.; Nathania, A.; Budiman, A.S. Mechanical Studies of Solar Photovoltaics (PV) Backsheets Under Salt Damp Heat Environments. *Procedia Eng.* **2017**, *215*, 238–245. [CrossRef]
140. Oreski, G.; Barretta, C.; Macher, A.; Eder, G.; Neumaier, L.; Feichtner, M.; Aarnio Winterhof, M. Investigation of the Crack Propensity of Co-Extruded Polypropylene Backsheet Films for Photovoltaic Modules. *Sol. Energy Mater. Sol. Cells* **2023**, *259*, 112438. [CrossRef]
141. Elfaqih, A.K.; Tawil, I.H. Mechanical Behavior Study of PPCF Material as Solar Photovoltaic Backsheet. In Proceedings of the 2022 IEEE 2nd International Maghreb Meeting of the Conference on Sciences and Techniques of Automatic Control and Computer Engineering, Sabrata, Libya, 23–25 May 2022; pp. 650–654.
142. Pascual, J.; García, M.; Marcos, J.; Marroyo, L. Analysis of polyamide and fluoropolymer backsheets: Degradation and insulation failure in field-aged photovoltaic modules. *Prog. Photovolt. Res. Appl.* **2023**, *31*, 494–505. [CrossRef]
143. Gebhardt, P.; Bauermann, L.P.; Philipp, D. Backsheet Chalking—Theoretical Background and Relation to Backsheet Cracking and Insulation Failures. In Proceedings of the 35th European Photovoltaic Solar Energy Conference and Exhibition, Brussels, Belgium, 24–28 September 2018; pp. 24–28.
144. Uličná, S.; Owen-Bellini, M.; Moffitt, S.L.; Sinha, A.; Tracy, J.; Roy-Choudhury, K.; Miller, D.C.; Hacke, P.; Schelhas, L.T. A study of degradation mechanisms in PVDF-based photovoltaic backsheets. *Sci. Rep.* **2022**, *12*, 14399. [CrossRef]
145. Xia, J.; Liu, Y.; Hu, H.; Zhu, X.; Lv, H.; Phillips, N.H.; Choudhury, K.R.; Gambogi, W.J.; Rodriguez, M.; Simon, E.S. Impact of specimen preparation method on photovoltaic backsheet degradation during accelerated aging test. *Energy Sci. Eng.* **2022**, *10*, 1961–1971. [CrossRef]
146. Mühleisen, W. Minimizing Crack Propagation in Cracked PV Backsheets with Repair Coatings. In Proceedings of the 8th World Conference on Photovoltaic Energy Conversion, Milan, Italy, 26–30 September 2022.
147. Beaucarne, G.; Eder, G.; Jadot, E.; Voronko, Y.; Mühleisen, W. Repair and preventive maintenance of photovoltaic modules with degrading backsheets using flowable silicone sealant. *Prog. Photovolt. Res. Appl.* **2022**, *30*, 1045–1053. [CrossRef]
148. Wu, Z.; Lyu, S.; Peng, Q.; Han, H.; Zhu, D. Thermomechanical Stress Distribution Analysis of Junction Box on Silicon Photovoltaic Modules Based on Finite Element Analysis. *IEEE J. Photovolt.* **2019**, *9*, 1716–1720. [CrossRef]
149. Diaz-Dorado, E.; Suárez-García, A.; Carrillo, C.; Cidras, J. Influence of the shadows in photovoltaic systems with different configurations of bypass diodes. In Proceedings of the SPEEDAM 2010, Pisa, Italy, 14–16 June 2010; pp. 134–139.
150. Bakır, H. A comparative evaluation and real-time measurement of failures in solar power plants by thermal imaging in Turkey. *Therm. Sci. Eng. Prog.* **2023**, *42*, 101945. [CrossRef]
151. Kim, M.-S.; Kim, D.-H.; Kim, H.-J.; Prabakar, K. A Novel Strategy for Monitoring a PV Junction Box Based on LoRa in a 3 kW Residential PV System. *Electronics* **2022**, *11*, 709. [CrossRef]
152. Brecl, K.; Pirc, M.; Bokalič, M.; Morelj, D.; Topič, M. PV module behaviour on the substring level under real conditions monitored by junction box electronic device Jubomer. *IET Renew. Power Gener.* **2019**, *13*, 2802–2806. [CrossRef]
153. Ong, N.A.F.M.N.; Sadiq, M.A.; Said, M.S.M.; Jomaas, G.; Tohir, M.Z.M.; Kristensen, J.S. Fault tree analysis of fires on rooftops with photovoltaic systems. *J. Build. Eng.* **2022**, *46*, 103752.
154. Daher, D.H.; Aghaei, M.; Quansah, D.A.; Adaramola, M.S.; Parvin, P.; Ménézo, C. Multi-pronged degradation analysis of a photovoltaic power plant after 9.5 years of operation under hot desert climatic conditions. *Prog. Photovolt. Res. Appl.* **2023**, *31*, 888–907. [CrossRef]
155. Vo, T.T.E.; Ko, H.; Huh, J.; Park, N. Overview of possibilities of solar floating photovoltaic systems in the offshore industry. *Energies* **2021**, *14*, 6988. [CrossRef]
156. Ghosh, A. A comprehensive review of water based PV: Flotavoltaics, under water, offshore & canal top. *Ocean Eng.* **2023**, *281*, 115044. [CrossRef]
157. Tabet, S.; Ihaddadene, R.; Guerira, B.; Ihaddadene, N. Impact of Dust and Degradation on the Electrical Properties of PV Panels. *J. Renew. Energy Environ.* **2023**, *10*, 78–88.
158. Xue-Yan, L.; Ji-Gao, Z. Dust corrosion. In Proceedings of the 50th IEEE Holm Conference on Electrical Contacts and the 22nd International Conference on Electrical Contacts Electrical Contacts, Seattle, WA, USA, 23 September 2004; pp. 255–262.
159. Karimi, M.; Samet, H.; Ghanbari, T.; Moshksar, E. A current based approach for hotspot detection in photovoltaic strings. *Int. Trans. Electr. Energy Syst.* **2020**, *30*, e12517. [CrossRef]
160. Kim, K.A.; Krein, P.T. Hot spotting and second breakdown effects on reverse IV characteristics for mono-crystalline Si photovoltaics. In Proceedings of the 2013 IEEE Energy Conversion Congress and Exposition, Denver, CO, USA, 15–19 September 2013; pp. 1007–1014.
161. AE-Solar. *Smart Modules with Hot-Spot Free Technology*; AE-Solar Alternative Energy: Bavaria, Germany, 2018.
162. Ross, R.G. PV reliability development lessons from JPL's flat plate solar array project. *IEEE J. Photovolt.* **2013**, *4*, 291–298. [CrossRef]
163. Oufettoul, H.; Motahhir, S.; Aniba, G.; Masud, M.; AlZain, M.A. Improved TCT topology for shaded photovoltaic arrays. *Energy Rep.* **2022**, *8*, 5943–5956. [CrossRef]

164. Spanoche, S.A.; Stewart, J.D.; Hawley, S.L.; Opris, I.E. Model-based method for partially shaded PV modules hot spot suppression. In Proceedings of the 2012 IEEE 38th Photovoltaic Specialists Conference (PVSC) PART 2, Austin, TX, USA, 3–8 June 2012; pp. 1–7.
165. Herrmann, W.; Wiesner, W.; Vaassen, W. Hot spot investigations on PV modules-new concepts for a test standard and consequences for module design with respect to bypass diodes. In Proceedings of the Conference Record of the Twenty Sixth IEEE Photovoltaic Specialists Conference, Anaheim, CA, USA, 29 September–3 October 1997; pp. 1129–1132.
166. Bakır, H. Detection of Faults in Photovoltaic Modules of SPPS in Turkey; Infrared Thermographic Diagnosis and Recommendations. *J. Electr. Eng. Technol.* **2023**, *18*, 1945–1957. [CrossRef]
167. Ghosh, S.; Singh, S.K.; Yadav, V.K. Experimental investigation of hotspot phenomenon in PV arrays under mismatch conditions. *Sol. Energy* **2023**, *253*, 219–230. [CrossRef]
168. Al Mahdi, H.A.; Leahy, P.G.; Morrison, A.P. Predicting Early EVA Degradation in Photovoltaic Modules From Short Circuit Current Measurements. *IEEE J. Photovolt.* **2021**, *11*, 1188–1196. [CrossRef]
169. Kuitche, J.M.; Pan, R.; TamizhMani, G. Investigation of Dominant Failure Mode(s) for Field-Aged Crystalline Silicon PV Modules under Desert Climatic Conditions. *IEEE J. Photovolt.* **2014**, *4*, 814–826. [CrossRef]
170. Hong, Y.-Y.; Pula, R.A. Methods of photovoltaic fault detection and classification: A review. *Energy Rep.* **2022**, *8*, 5898–5929. [CrossRef]
171. Tanaka, K.; Matsumoto, K.I.; Keeley, A.R.; Managi, S. The impact of weather changes on the supply and demand of electric power and wholesale prices of electricity in Germany. *Sustain. Sci.* **2022**, *17*, 1813–1825. [CrossRef]
172. Tripathi, A.K.; Aruna, M.; Murthy, C.S.N. Output power loss of photovoltaic panel due to dust and temperature. *Int. J. Renew. Energy Res.* **2017**, *7*, 439–442.
173. Hasan, K.; Yousuf, S.B.; Tushar, M.S.H.K.; Das, B.K.; Das, P.; Islam, M.S. Effects of different environmental and operational factors on the PV performance: A comprehensive review. *Energy Sci. Eng.* **2022**, *10*, 656–675. [CrossRef]
174. Santhakumari, M.; Sagar, N. A review of the environmental factors degrading the performance of silicon wafer-based photovoltaic modules: Failure detection methods and essential mitigation techniques. *Renew. Sustain. Energy Rev.* **2019**, *110*, 83–100. [CrossRef]
175. Abdallah, A.A.; Ali, K.; Kivambe, M.M.; Darussalam, B. Common failure modes observed in PV system installed in desert climate. *Sol. Energy* **2023**, *249*, 268–277. [CrossRef]
176. Zaihidee, F.M.; Mekhilef, S.; Seyedmahmoudian, M.; Horan, B. Dust as an unalterable deteriorative factor affecting PV panel's efficiency: Why and how. *Renew. Sustain. Energy Rev.* **2016**, *65*, 1267–1278. [CrossRef]
177. Saidan, M.; Albaali, A.G.; Alasis, E.; Kaldellis, J.K. Experimental study on the effect of dust deposition on solar photovoltaic panels in desert environment. *Renew. Energy* **2016**, *92*, 499–505. [CrossRef]
178. Mehmood, U.; Al-Sulaiman, F.A.; Yilbas, B. Characterization of dust collected from PV modules in the area of Dhahran, Kingdom of Saudi Arabia, and its impact on protective transparent covers for photovoltaic applications. *Sol. Energy* **2017**, *141*, 203–209. [CrossRef]
179. Fan, S.; Wang, Y.; Cao, S.; Sun, T.; Liu, P. A novel method for analyzing the effect of dust accumulation on energy efficiency loss in photovoltaic (PV) system. *Energy* **2021**, *234*, 121112. [CrossRef]
180. Said, S.A.M.; Walwil, H.M. Fundamental studies on dust fouling effects on PV module performance. *Sol. Energy* **2014**, *107*, 328–337. [CrossRef]
181. Sayigh, A.; Al-Jandal, S.; Ahmed, H. Dust effect on solar flat surfaces devices in Kuwait. In Proceedings of the Workshop on the Physics of Non-Conventional Energy Sources and Materials Science for Energy, Miramare-Trieste, Italy, 2–20 September 1985; pp. 353–367.
182. Elminir, H.K.; Ghitas, A.E.; Hamid, R.; El-Hussainy, F.; Beheary, M.; Abdel-Moneim, K.M. Effect of dust on the transparent cover of solar collectors. *Energy Convers. Manag.* **2006**, *47*, 3192–3203. [CrossRef]
183. Kazem, H.A.; Chaichan, M.T.; Al-Waeli, A.H.A.; Al-Badi, R.; Fayad, M.A.; Gholami, A. Dust impact on photovoltaic/thermal system in harsh weather conditions. *Sol. Energy* **2022**, *245*, 308–321. [CrossRef]
184. Yazdani, H.; Yaghoubi, M. Dust deposition effect on photovoltaic modules performance and optimization of cleaning period: A combined experimental–numerical study. *Sustain. Energy Technol. Assess.* **2022**, *51*, 101946. [CrossRef]
185. Sharif, M.A.; Rashid, M.; Korkmaz, F. Effects of Weather and Environmental Conditions on the Power Productivity of Photovoltaic Module in Kirkuk City. *NTU J. Renew. Energy* **2023**, *4*, 1–6.
186. Fu, X.; Wang, X.; Gong, Y.; Wang, Y.; Zhang, Y. Impact of Snow Weather on PV Power Generation and Improvement of Power Forecasting. In Proceedings of the 2023 International Conference on Power Energy Systems and Applications (ICoPESA), Chengdu, China, 24–26 February 2023; pp. 448–453.
187. Bahanni, C.; Adar, M.; Boulmrharj, S.; Khaidar, M.; Mabrouki, M. Performance comparison and impact of weather conditions on different photovoltaic modules in two different cities. *Indones. J. Electr. Eng. Comput. Sci.* **2022**, *25*, 1275–1286. [CrossRef]
188. Mellit, A.; Tina, G.M.; Kalogirou, S.A. Fault detection and diagnosis methods for photovoltaic systems: A review. *Renew. Sustain. Energy Rev.* **2018**, *91*, 1–17. [CrossRef]
189. Standard, I.E.C. 61215 Crystalline Silicon Terrestrial Photovoltaic (PV) Modules Design Qualification and Type Approval. *Int. Electrotech. Comm.* **1995**. Available online: https://webstore.iec.ch/publication/68594&preview (accessed on 9 February 2022).
190. Kumar, N.M.; Sudhakar, K.; Samykano, M.; Jayaseelan, V. On the technologies empowering drones for intelligent monitoring of solar photovoltaic power plants. *Procedia Comput. Sci.* **2018**, *133*, 585–593. [CrossRef]

191. Buerhop, C.; Bommes, L.; Schlipf, J.; Pickel, T.; Fladung, A.; Peters, M. Infrared imaging of photovoltaic modules A review of the state of the art and future challenges facing gigawatt photovoltaic power stations. *Prog. Energy* **2022**, *4*, 042010. [CrossRef]
192. Goodarzi, D.M.; Lauri, J.; Putaala, J.; Nousiainen, O.; Fabritius, T. Eddy current soldering of solar cell ribbons under a layer of glass. *Sol. Energy Mater. Sol. Cells* **2023**, *259*, 112427. [CrossRef]
193. Drabczyk, K.; Kulesza-Matlak, G.; Drygała, A.; Szindler, M.; Lipiński, M. Electroluminescence imaging for determining the influence of metallization parameters for solar cell metal contacts. *Sol. Energy* **2016**, *126*, 14–21. [CrossRef]
194. Hobbs, W.; Lavrova, O.; Lockridge, B. *Comparison of Electroluminescence Image Capture Methods*; Sandia National Lab. (SNL-NM): Albuquerque, NM, USA, 2016.
195. Høiaas, I.; Grujic, K.; Imenes, A.G.; Burud, I.; Olsen, E.; Belbachir, N. Inspection and condition monitoring of large-scale photovoltaic power plants: A review of imaging technologies. *Renew. Sustain. Energy Rev.* **2022**, *161*, 112353. [CrossRef]
196. Kajari-Schröder, S.; Kunze, I.; Eitner, U.; Köntges, M. Spatial and orientational distribution of cracks in crystalline photovoltaic modules generated by mechanical load tests. *Sol. Energy Mater. Sol. Cells* **2011**, *95*, 3054–3059. [CrossRef]
197. Dallas, W.; Polupan, O.; Ostapenko, S. Resonance ultrasonic vibrations for crack detection in photovoltaic silicon wafers. *Meas. Sci. Technol.* **2007**, *18*, 852. [CrossRef]
198. Belyaev, A.; Polupan, O.; Dallas, W.; Ostapenko, S.; Hess, D.; Wohlgemuth, J. Crack detection and analyses using resonance ultrasonic vibrations in full-size crystalline silicon wafers. *Appl. Phys. Lett.* **2006**, *88*, 111907. [CrossRef]
199. Hamid, S.A.; Zulkifli, M.N. Microstructure Evaluation of Photovoltaic Solar Panel's Interconnection: A Review. *Mater. Sci. Forum* **2022**, *1055*, 27–35. [CrossRef]
200. Rifat, A.; Pandao, P.P.; Babu, B.S. Solar Powered Fault Detection System for Railway Tracks. *Eur. J. Electr. Eng. Comput. Sci.* **2022**, *6*, 39–43. [CrossRef]
201. Pillai, D.S.; Rajasekar, N. Metaheuristic algorithms for PV parameter identification: A comprehensive review with an application to threshold setting for fault detection in PV systems. *Renew. Sustain. Energy Rev.* **2018**, *82*, 3503–3525. [CrossRef]
202. Chockalingam, A.; Naveen, S.; Sanjay, S.; Nanthakumar, J.; Praveenkumar, V. *Sensor Based Hotspot Detection and Isolation in Solar Array System Using IOT*; Renewable Energy Lab, Prince Sultan University: Riyadh, Saudi Arabia, 2023; pp. 371–376.
203. Lee, H.-M.; Chae, W.-K.; Kim, W.-H.; Kim, J.-E. Cooperative Use of IMD and GPT in a 3-Phase Ungrounded Distribution System Linked to a Transformerless Photovoltaic Power Generation Facility. *Appl. Sci.* **2023**, *13*, 1558. [CrossRef]
204. Meribout, M.; Tiwari, V.K.; Herrera, J.P.P.; Baobaid, A.N.M.A. Solar panel inspection techniques and prospects. *Measurement* **2023**, *209*, 112466. [CrossRef]
205. Garoudja, E.; Harrou, F.; Sun, Y.; Kara, K.; Chouder, A.; Silvestre, S. Statistical fault detection in photovoltaic systems. *Sol. Energy* **2017**, *150*, 485–499. [CrossRef]
206. Harrou, F.; Sun, Y.; Taghezouit, B.; Saidi, A.; Hamlati, M.-E. Reliable fault detection and diagnosis of photovoltaic systems based on statistical monitoring approaches. *Renew. Energy* **2018**, *116*, 22–37. [CrossRef]
207. Ali, M.H.; Rabhi, A.; El Hajjaji, A.; Tina, G.M. Real time fault detection in photovoltaic systems. *Energy Procedia* **2017**, *111*, 914–923. [CrossRef]
208. Mustafa, Z.; Awad, A.S.A.; Azzouz, M.; Azab, A. Fault identification for photovoltaic systems using a multi-output deep learning approach. *Expert Syst. Appl.* **2023**, *211*, 118551. [CrossRef]
209. Lodhi, E.; Wang, F.-Y.; Xiong, G.; Zhu, L.; Tamir, T.S.; Rehman, W.U.; Khan, M.A. A Novel Deep Stack-Based Ensemble Learning Approach for Fault Detection and Classification in Photovoltaic Arrays. *Remote Sens.* **2023**, *15*, 1277. [CrossRef]
210. Garoudja, E.; Chouder, A.; Kara, K.; Silvestre, S. An enhanced machine learning based approach for failures detection and diagnosis of PV systems. *Energy Convers. Manag.* **2017**, *151*, 496–513. [CrossRef]
211. Chen, L.; Li, S.; Wang, X. Quickest fault detection in photovoltaic systems. *IEEE Trans. Smart Grid* **2016**, *9*, 1835–1847. [CrossRef]
212. Chine, W.; Mellit, A.; Lughi, V.; Malek, A.; Sulligoi, G.; Pavan, A.M. A novel fault diagnosis technique for photovoltaic systems based on artificial neural networks. *Renew. Energy* **2016**, *90*, 501–512. [CrossRef]
213. Et-taleby, A.; Chaibi, Y.; Benslimane, M.; Boussetta, M. Applications of Machine Learning Algorithms for Photovoltaic Fault Detection: A Review. *Stat. Optim. Inf. Comput.* **2023**, *11*, 168–177. [CrossRef]
214. Li, B.; Delpha, C.; Diallo, D.; Migan-Dubois, A. Application of Artificial Neural Networks to photovoltaic fault detection and diagnosis: A review. *Renew. Sustain. Energy Rev.* **2021**, *138*, 110512. [CrossRef]
215. Abubakar, A.; Almeida, C.F.M.; Gemignani, M. Review of artificial intelligence-based failure detection and diagnosis methods for solar photovoltaic systems. *Machines* **2021**, *9*, 328. [CrossRef]
216. Kurukuru, V.S.B.; Haque, A.; Khan, M.A.; Sahoo, S.; Malik, A.; Blaabjerg, F. A review on artificial intelligence applications for grid-connected solar photovoltaic systems. *Energies* **2021**, *14*, 4690. [CrossRef]
217. Tina, G.M.; Ventura, C.; Ferlito, S.; De Vito, S. A state-of-art-review on machine-learning based methods for PV. *Appl. Sci.* **2021**, *11*, 7550. [CrossRef]
218. Cotfas, D.T.; Cotfas, P.A.; Kaplanis, S. Methods to determine the dc parameters of solar cells: A critical review. *Renew. Sustain. Energy Rev.* **2013**, *28*, 588–596. [CrossRef]
219. Pan, J.-S.; Tian, A.-Q.; Pan, T.-S.; Chu, S.-C. Parameters Extraction of Solar Cell Using an Improved QUasi-Affine TRansformation Evolution (QUATRE) Algorithm. In *Advances in Intelligent Systems and Computing*; Springer: Berlin/Heidelberg, Germany, 2022; pp. 253–263.

220. Qin, J.; Wang, L.; Yang, S.; Huang, R. The effect of solar cell shunt resistance change on the bus voltage ripple in spacecraft power system. *Microelectron. Reliab.* **2018**, *88*, 1047–1050. [CrossRef]
221. d'Alessandro, V.; Guerriero, P.; Daliento, S.; Gargiulo, M. A straightforward method to extract the shunt resistance of photovoltaic cells from current–voltage characteristics of mounted arrays. *Solid-State Electron.* **2011**, *63*, 130–136. [CrossRef]
222. Kim, Y.S.; Kang, S.-M.; Johnston, B.; Winston, R. A novel method to extract the series resistances of individual cells in a photovoltaic module. *Sol. Energy Mater. Sol. Cells* **2013**, *115*, 21–28. [CrossRef]
223. Lucheng, Z.; Hui, S. Novel approach for characterizing the specific shunt resistance caused by the penetration of the front contact through the p–n junction in solar cell. *J. Semicond.* **2009**, *30*, 074007. [CrossRef]
224. Mohapatra, A.; Nayak, B.; Mohanty, K. Parameter Extraction of PV Module using NLS Algorithm with Experimental Validation. *Int. J. Electr. Comput. Eng.* **2017**, *7*, 2392. [CrossRef]
225. Elyaqouti, M.; Saadaoui, D.; Lidaighbi, S.; Chaoufi, J.; Ibrahim, A.; Aqel, R.; Obukhov, S. A novel hybrid numerical with analytical approach for parameter extraction of photovoltaic modules. *Energy Convers. Manag. X* **2022**, *14*, 100219.
226. Meena, R.; Niyaz, H.M.; Gupta, R. Investigation and Differentiation of Degradation Modes Affecting Series Resistance in Photovoltaic Cells and Modules. *IEEE J. Photovolt.* **2023**, *13*, 283–290. [CrossRef]
227. Ramalingam, K.; Indulkar, C.; Gharehpetian, G.B.; Mousavi Agah, S.M. Chapter 3—Solar Energy and Photovoltaic Technology. In *Distributed Generation Systems*; Butterworth-Heinemann: Oxford, UK, 2017; pp. 69–147.
228. Roy, S.; Gupta, R. Quantitative Estimation of Shunt Resistance in Crystalline Silicon Photovoltaic Modules by Electroluminescence Imaging. *IEEE J. Photovolt.* **2019**, *9*, 1741–1747. [CrossRef]
229. Kaplanis, S.; Kaplani, E. Energy performance and degradation over 20 years performance of BP c-Si PV modules. *Simul. Model. Pract. Theory* **2011**, *19*, 1201–1211. [CrossRef]
230. Dhass, A.D.; Beemkumar, N.; Harikrishnan, S.; Ali, H.M. A Review on Factors Influencing the Mismatch Losses in Solar Photovoltaic System. *Int. J. Photoenergy* **2022**, *2022*, 2986004. [CrossRef]
231. Sinha, A.; Sastry, O.; Gupta, R. Nondestructive characterization of encapsulant discoloration effects in crystalline-silicon PV modules. *Sol. Energy Mater. Sol. Cells* **2016**, *155*, 234–242. [CrossRef]
232. Lin, L.; Bora, B.; Prasad, B. Influence of outdoor conditions on PV module performance—An overview. *Mater. Sci. Eng.* **2023**, *7*, 88–101.
233. Pavlík, M.; Beňa, L.U.; Medved', D.; Čonka, Z.; Kolcun, M. Analysis and evaluation of photovoltaic cell defects and their impact on electricity generation. *Energies* **2023**, *16*, 2576. [CrossRef]
234. Gxasheka, A.R.; Van Dyk, E.E.; Meyer, E.L. Evaluation of performance parameters of PV modules deployed outdoors. *Renew. Energy* **2005**, *30*, 611–620. [CrossRef]
235. Rajput, P.; Malvoni, M.; Kumar, N.M.; Sastry, O.S.; Tiwari, G.N. Risk priority number for understanding the severity of photovoltaic failure modes and their impacts on performance degradation. *Case Stud. Therm. Eng.* **2019**, *16*, 100563. [CrossRef]
236. Ruschel, C.S.; Gasparin, F.P.; Costa, E.R.; Krenzinger, A. Assessment of PV modules shunt resistance dependence on solar irradiance. *Sol. Energy* **2016**, *133*, 35–43. [CrossRef]
237. Zhang, J.; Liu, Y.; Ding, K.; Feng, L.; Hamelmann, F.U.; Chen, X. Model Parameter Analysis of Cracked Photovoltaic Module under Outdoor Conditions. In Proceedings of the 2020 47th IEEE Photovoltaic Specialists Conference (PVSC), Calgary, ON, Canada, 15 June 2020; pp. 2509–2512.
238. Oh, J.; Bowden, S.; TamizhMani, G. Potential-induced degradation (PID): Incomplete recovery of shunt resistance and quantum efficiency losses. *IEEE J. Photovolt.* **2015**, *5*, 1540–1548. [CrossRef]
239. Luo, W.; Khoo, Y.S.; Hacke, P.; Naumann, V.; Lausch, D.; Harvey, S.P.; Singh, J.P.; Chai, J.; Wang, Y.; Aberle, A.G. Potential-induced degradation in photovoltaic modules: A critical review. *Energy Environ. Sci.* **2017**, *10*, 43–68. [CrossRef]
240. Hacke, P.; Spataru, S.; Johnston, S.; Terwilliger, K.; VanSant, K.; Kempe, M.; Wohlgemuth, J.; Kurtz, S.; Olsson, A.; Propst, M. Elucidating PID Degradation Mechanisms and In Situ Dark I–V Monitoring for Modeling Degradation Rate in CdTe Thin-Film Modules. *IEEE J. Photovolt.* **2016**, *6*, 1635–1640. [CrossRef]
241. Dhass, A.D.; Natarajan, E.; Ponnusamy, L. Influence of shunt resistance on the performance of solar photovoltaic cell. In Proceedings of the 2012 International Conference on Emerging Trends in Electrical Engineering and Energy Management (ICETEEEM), Tiruchirapalli, India, 13–15 December 2012; pp. 382–386.
242. van Dyk, E.E.; Meyer, E.L. Analysis of the effect of parasitic resistances on the performance of photovoltaic modules. *Renew. Energy* **2004**, *29*, 333–344. [CrossRef]
243. Sarkar, M.N.I. Effect of various model parameters on solar photovoltaic cell simulation: A SPICE analysis. *Renew. Wind Water Sol.* **2016**, *3*, 1–9. [CrossRef]
244. Kennerud, K.L. Analysis of performance degradation in CdS solar cells. *IEEE Trans. Aerosp. Electron. Syst.* **1969**, 912–917. [CrossRef]
245. Rummel, S.R.; McMahon, T.J. Effect of cell shunt resistance on PV module performance at reduced light levels. *AIP Conf. Proc.* **1996**, *353*, 581–586.
246. Al Mahdi, H. Predicting Photovoltaic Module Degradation Using Current-Voltage. Ph.D. Dissertation, University College Cork, Cork, Ireland, 2022. Available online: https://hdl.handle.net/10468/13282 (accessed on 10 September 2023).
247. Al Mahdi, H.; Leahy, P.G.; Morrison, A.P. Experimentally derived models to detect onset of shunt resistance degradation in photovoltaic modules. *Energy Rep.* **2023**, *10*, 604–612. [CrossRef]

248. Hussain, T.; Hussain, M.; Al-Aqrabi, H.; Alsboui, T.; Hill, R. A Review on Defect Detection of Electroluminescence-Based Photovoltaic Cell Surface Images Using Computer Vision. *Energies* **2023**, *16*, 4012. [CrossRef]
249. Zamzeer, A.S.; Farhan, M.S.; Rikabi, H.T.S.A. An Investigation into Faults of PV system using Machine Learning: A Systematic Review. In Proceedings of the 2023 Third International Conference on Advances in Electrical, Computing, Communication and Sustainable Technologies (ICAECT), Bhilai, Chhattisgarh, India, 5–6 January 2023; pp. 1–6.
250. Mansouri, M.; Trabelsi, M.; Nounou, H.; Nsounou, M. Deep Learning-Based Fault Diagnosis of Photovoltaic Systems: A Comprehensive Review and Enhancement Prospects. *IEEE Access* **2021**, *9*, 126286–126306. [CrossRef]
251. Zeb, K.; Islam, S.U.; Khan, I.; Uddin, W.; Ishfaq, M.; Curi Busarello, T.D.; Muyeen, S.M.; Ahmad, I.; Kim, H.J. Faults and Fault Ride through strategies for grid-connected photovoltaic system: A comprehensive review. *Renew. Sustain. Energy Rev.* **2022**, *158*, 112125. [CrossRef]